Submitted to Angewandte Chemie International Edition as a Communication

Iron(II) Catalyzed Hydrophosphination of Isocyanates

Helen R. Sharpe, Ana M. Geer, William Lewis, Alexander J. Blake and Deborah L. Kays*

Abstract: The first transition metal catalyzed hydrophosphination of isocyanates is presented. The use of low-coordinate iron(II) precatalysts leads to an unprecedented catalytic double insertion of isocyanates into the P-H bond of diphenylphosphine to yield phosphinodicarboxamides [$Ph_2PC(=O)N(R)C(=O)N(H)R$], a new family of derivatized organophosphorus compounds. This remarkable result can be attributed to the low-coordinate nature of the iron(II) centres whose inherent electron deficiency enables a Lewis-acid mechanism in which a combination of the steric pocket of the metal centre and substrate size determines the reaction products and regioselectivity.

Organophosphorus compounds are a vital class of chemicals with extensive commercial applications.[1] Classic synthetic methodologies for phosphine preparation have major drawbacks; including poor functional group tolerance, side-product formation, the use of protecting groups and stoichiometric amounts of additives, which is a significant disadvantage for atom economy.[2] Therefore, there is growing demand to develop atom-economical routes for the preparation of functionalized phosphines. In particular, hydrophosphination is an attractive synthetic route to phosphine products, proceeding *via* P-H bond addition across a C-C/X (X = O, N, S) multiple bond.[3] However, this reaction can be synthetically challenging as a result of the coordination capability of both the phosphine substrates and products which can poison the metal catalyst.

The hydrophosphination of olefins and alkynes has received wide attention in the last decade,[4] but the use of heterocumulene substrates has been less explored, with examples of precatalysts for these reactions limited to rare-earth,[5] alkali metal,[6] and group 2 complexes.[7] The hydrophosphination of organic isocyanates, yielding phosphinocarboxamide products, is limited to a few recent examples, all of which are catalyzed by f-block complexes.[5a-c, 5e] A significant issue with the hydrophosphination of isocyanates is that of competing side reactions, such as the cyclotrimerization of isocyanates to isocyanurates and catalyst incompatibility towards heteroatom-containing substrates. This This catalyst incompatibility has been documented for the hydrophosphination of aromatic substrates using $LY[N(SiMe_3)_2]_2$ (L = [4-CH_3-2-{(CH_3)CH-[$N(CH)_2CN$]}C_6H_3]$_2$N).[5c]

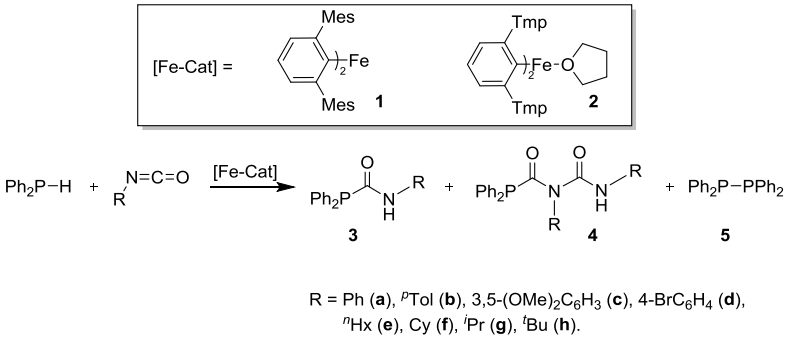

Scheme 1. Hydrophosphination of isocyanates with Ph_2PH catalyzed by **1** and **2**.

Herein, we report the first transition metal-catalyzed hydrophosphination of isocyanates, which affords phosphinodicarboxamides *via* an unprecedented catalytic double insertion of isocyanates into the P–H bond of the phosphine. The reaction between organic isocyanates and diphenylphosphine in the presence of catalytic amounts of (2,6-$Mes_2C_6H_3$)$_2$Fe[8] (**1**; Mes = 2,4,6-

$Me_3C_6H_2$) or (2,6-$Tmp_2C_6H_3$)$_2$Fe(THF)[9] (**2**; Tmp = 2,4,5-$Me_3C_6H_2$) produces the mono- (**3**) and/or diinsertion (**4**) products, where one or two isocyanate units have inserted into the P-H bond respectively (Scheme 1). This result is remarkable since diinsertion processes are incredibly rare.[10] Significantly, compounds **4** are a new family of derivatized phosphinodicarboxamides with potential applications in coordination chemistry,[11] supramolecular and self-assembled arrays,[12] in biomedicine [13] and enantioselective catalysis.[14]

Table 1. Catalytic hydrophosphination of isocyanates mediated by **1** and **2**.[a]

Entry	RNCO	Cat.	RNCO: Ph_2PH	t (h)	Conv. (%)[b]	**3**/**4**/**5** (%)[c]
1	Ph	**1**	1:1	16	98	59/41/0
2	Ph	**1**	2:1	15	95	33/67/0
3	Ph	**2**	2:1	6	96	35/65/0
4	*p*Tol	**1**	2:1	16.5	95	27/72/1
5	*p*Tol	**2**	2:1	4.8	94	36/63/1
6	$(OMe)_2C_6H_3$	**1**	2:1	12	95	43/57/0
7	$(OMe)_2$ C_6H_3	**2**	2:1	3	99	46/54/0
8	4-BrC_6H_4	**1**	2:1	15	99	30/70/0
9	4-BrC_6H_4	**2**	2:1	4	99	27/71/2
10	*n*Hx	**1**	1:1	15	99	13/26/5/56[d]
11	*n*Hx	**1**	2:1	15	99	8/39/3/49[d]
12	*n*Hx	**2**	2:1	15	99	12/36/7/46[d]
13	Cy	**1**	1:1	16	90	93/0/6[e]
14	Cy	**2**	1:1	8	89	95/0/5
15	*i*Pr	**1**	1:1	16	55	91/5/4
16	*i*Pr	**1**[f]	1:1	1.6	89	96/0/4
17	*i*Pr	**2**[f]	1:1	1	92	97/0/3
18	*t*Bu	**1**[f]	1:1	16	70	91/0/9
19	*t*Bu	**2**[f]	1:1	16	77	86/0/14

[a] Reaction conditions: 10 mg cat. (5 mol%), 0.6 mL of C_6D_6, 25 °C. [b] Determined by ^{1}H NMR and ^{31}P{^{1}H} NMR spectroscopy. [c] Ratio by ^{1}H NMR and ^{31}P{^{1}H} NMR. [d] Cyclotrimer ratio. [e] 1% unidentified ^{31}P{^{1}H} peak. [f] Catalysis performed at 60 °C.

Initially, Ph_2PH was treated with one equivalent of PhNCO using 5 mol% of **1** as the precatalyst (entry 1, Table 1). After 16 hours at room temperature, the solution underwent a colour change from yellow to dark red, with concomitant formation of two phosphorous-containing products as observed by ^{1}H and ^{31}P{^{1}H} NMR in a relative ratio of 59:41 (98% conversion). Further analysis revealed that the major product was [Ph_2PC(=O)N(H)Ph] (**3a**), while the second product was [Ph_2C(=O)N(Ph)C(=O)N(H)Ph] (**4a**), resulting from the double insertion of two isocyanate molecules into the P□H bond of Ph_2PH. In order to optimise the formation of **4a** the ratio of PhNCO:Ph_2PH was changed from 1:1 to 2:1 (entry 2, Table 1), resulting in an increase in the ratio of **4a** (67%) with respect to **3a** (33%). Three-coordinate complex **2** shows a higher activity than **1**; high conversion is achieved in a significantly shorter time with a similar product distribution (entry 3, Table 1). Very similar behaviour is observed for *p*TolNCO (entries 4 and 5, Table 1). When 3,5-$(OMe)_2C_6H_3$NCO is

used the hydrophosphination proceeds with a higher reaction rate and a small decrease in the amount of the diinsertion product (entries 6 and 7, Table 1). Reactions with isocyanates featuring functional groups proceed in a similar manner, with excellent conversions for substrates which bear either electron donating or withdrawing groups (entries 6-9, Table 1).

To explore the scope of the reaction aliphatic isocyanates were tested. When the reaction was performed with ^{n}HxNCO, the hydrophosphination competes with the cyclotrimerization reaction leading to a mixture of [^{n}HxNCO]$_3$,[9] [$Ph_2PC(=O)N(H)^{n}Hx$] (**3e**) and [$Ph_2PC(=O)N(^{n}Hx)C(=O)N(H)^{n}Hx$] (**4e**) (entries 10-12, Table 1). Meanwhile, reactions with more sterically encumbered secondary and tertiary isocyanates (CyNCO, ^{i}PrNCO and ^{t}BuNCO) afforded almost exclusively the monoinsertion products (**3f**-**h**, entries 13-19, Table 1). For ^{i}PrNCO and ^{t}BuNCO the temperature was raised to 60 °C in order to reach reasonable conversions in 16 h (entries 15-19, Table 1) *viz. ca.* 90% for **3g** and >70% for **3h**; previous attempts by others to catalyze the hydrophosphination of ^{t}BuNCO with Ph_2PH were low yielding (<20%).[5e] Collectively, these results indicate that the observed selectivity between the catalysis of the mono- and diinsertion of isocyanates into Ph_2PH may be governed by steric factors obtaining preferentially the diinsertion product for less bulky isocyanates and the monoinsertion product for secondary and tertiary aliphatic isocyanates.

Changing the solvent from C_6D_6 to THF resulted in a significant change in the selectivity (Table S1 and Scheme 2); affording the monoinsertion product almost exclusively. A decrease in catalyst activity was also observed, and the reactions required heating to 60 °C to obtain moderate conversions (entries 1-4, Table S1).

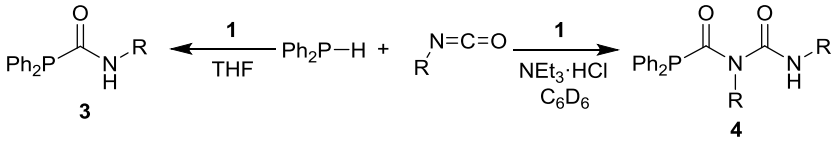

Scheme 2. Hydrophosphination products obtained when using THF (left) or NEt_3·HCl in C_6D_6 (right) catalyzed with 5 mol% of **1**.

To investigate the faster rates for precatalyst **2** compared to **1** the hydrophosphination catalysis was monitored using ^{1}H and ^{31}P{^{1}H} NMR spectroscopy. When using **1**, an induction period of around 2 h was observed (Figure 1, and ESI), indicating that the two-coordinate complex **1** is not the true catalyst and that a transformation takes place before the catalysis begins. No induction period is observed for **2**, where the catalysis starts immediately after substrate addition. It is likely that the same initial reaction takes place for **2** but the labile THF ligand is easily displaced making this step considerably faster. Surprisingly, when complex **1** was reacted separately with either Ph_2PH or CyNCO no reaction was observed after 48 h at room temperature by NMR and IR spectroscopy. As soon as the other substrate is added the formation of product **3f** is observed. Stoichiometric studies were not conclusive as IR spectroscopy shows several peaks in the amide region, but indicates that the active catalyst is an iron amidate complex (Scheme 3, **A**). The formation of this species could be an equilibrium; therefore both Ph_2PH and CyNCO are needed to drive the reaction

to **A**. However, the possibility that both substrates are required for precatalyst activation cannot be ruled out.

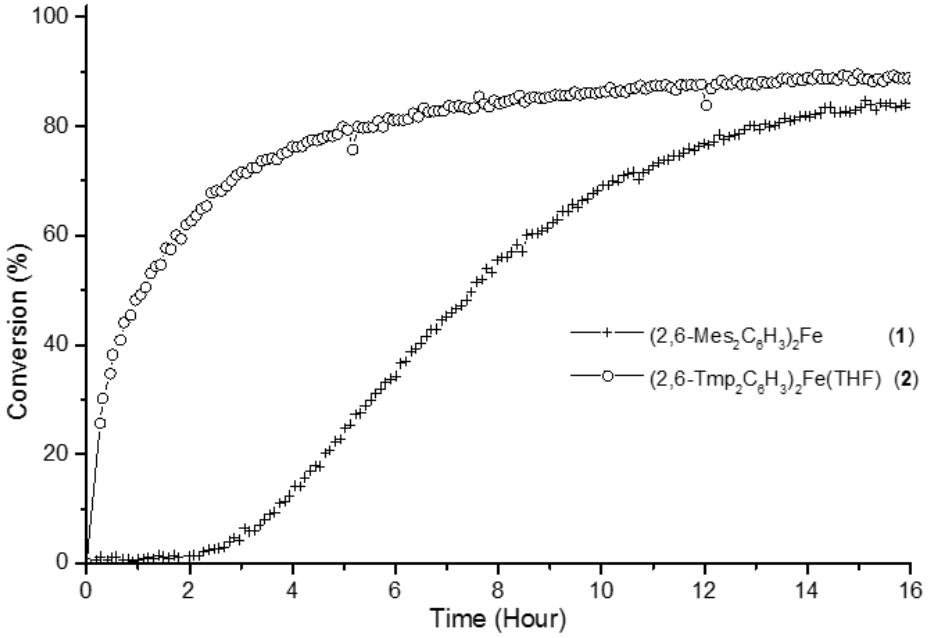

Figure 1. Conversion (%) *vs.* time (h) for the hydrophosphination of CyNCO with 5 mol% cat. of **1** (+) and **2** (○) in C_6D_6 at 25 °C.

Sigmoidal reaction kinetics have been used as evidence for a heterogeneous mechanism where the catalyst may be bulk iron metal or trace iron nanoclusters.[15] In order to distinguish the true nature of the catalyst, poisoning Fe with Hg and CS_2 were performed (see ESI). No change was observed in either the reaction rate or catalyst selectivity suggesting that the reaction most likely occurs through a homogenous mechanism. Moreover, the reaction does not appear to be radical catalyzed since the presence of excess cumene does not affect the rate of the reaction (see ESI).[16] No significant changes were observed when triethylamine was added to the reaction mixture (entry 1, Table S2). The addition of a weak acid (NEt_3·HCl) favours the double insertion product affording **4a** and **4c** almost exclusively (entries 2 and 4, Table S2 and Scheme 2), highlighting the mechanistic differences between our catalytic system and traditional palladium catalysts.[17]

With these mechanistic considerations in mind the proposed catalytic cycle is shown in Scheme 3. Due to the relatively high oxidation state of the iron(II) and its coordinative unsaturation it is conceivable to envisage the metal centre acting as a Lewis acid.[4e, 18] Therefore, a likely first step is the coordination of an isocyanate molecule leading to intermediate **B**. Nucleophilic attack of free Ph_2PH on the coordinated isocyanate leads to P-C bond formation and the transient species **C**. Similar substrate coordination followed by outer-sphere attack of a phosphine have been proposed.[4e, 19] A 1,3-proton shift, followed by addition of a new molecule of isocyanate regenerates the active species **B** with displacement of **3**. When the phosphinocarboxamide (**3**) produced in cycle 1 contains a smaller R group it is also possible to proceed into cycle 2 *via* a nucleophilic attack on **B** with the subsequent formation of **D**. Proton transfer followed by displacement of the phosphinodicarboxamide (**4**) by an incoming isocyanate molecule results in the regeneration of **B**. When coordinating solvents such as THF are used, solvation of intermediate **B** can occur blocking the income of a phosphinocarboxamide molecule enforcing the monoinsertion pathway. The weak acid will likely aid the protonolysis step in cycle 2; a rate limiting step for hydroamination reactions.[20] Indeed, when a mixture of PhNCO and CyNCO are reacted with diphenylphosphine (1:1:1) a combination of four products **3a**/**3f**/**4a**/**4i** are obtained (Scheme S1, ESI). The diinsertion product **4i**

[$Ph_2PC(=O)N(Ph)C(=O)NH(Cy)$] results from the coordination of CyNCO with nucleophilic attack of [$Ph_2PC(=O)N(H)Ph$] (**3a**) which is in agreement with our proposed mechanism.

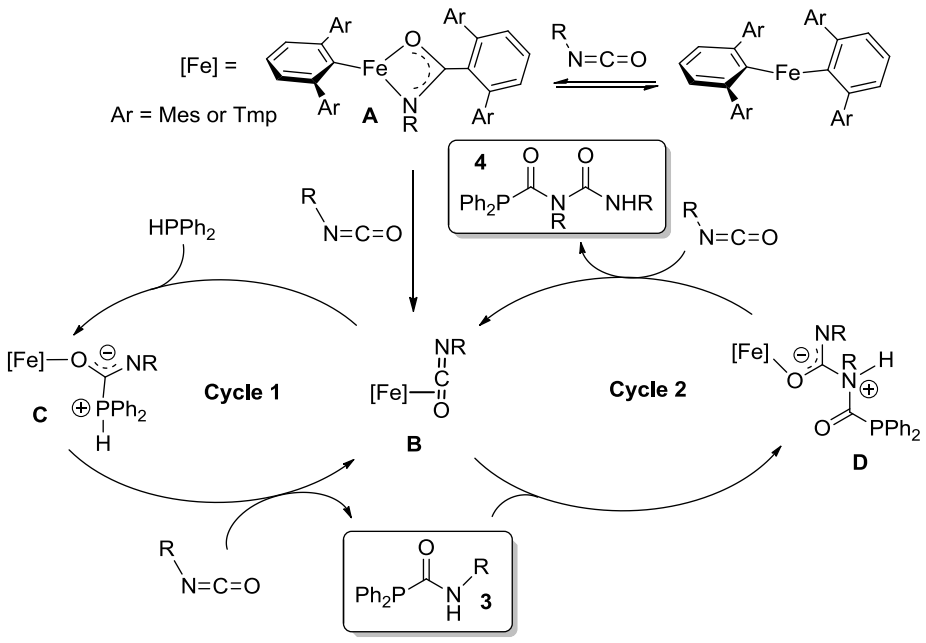

Scheme 3. Proposed mechanism for the mono- and diinsertion of isocyanates into the P-H bond of Ph_2PH.

An alternate mechanism similar to those reported for rare-earth precatalysts[5a,b,e] where the Ph_2PH attacks the metal centre first through protolytic cleavage of the amide ligand has been dismissed due to the lack of evidence of the formation of (2,6-$MesC_6H_3$)C(=O)NH(R) *via* ^{1}H NMR or IR spectroscopy.

Reactions were scaled up successfully obtaining good isolated yields for the diinsertion products (**4a**-**d**) and for monoinsertion products (**3a,c**-**d,f**-**h**) (see ESI for full procedures).

In summary, the catalytic hydrophosphination of isocyanates under mild conditions has been demonstrated using iron precatalysts **1** and **2**, which display remarkable reactivity due to their low coordination number and the unique steric pocket created by the bulky *m*-terphenyl ligands. Simple modification of the reaction conditions can control the synthetic outcome yielding either mono- or diinsertion products with high selectivity.

Acknowledgements

We gratefully acknowledge the support of the University of Nottingham, the EPSRC and Leverhulme Trust. We also thank Dr Ross Denton, University of Nottingham for mechanistic discussions, Dr Huw Williams, University of Nottingham for helpful NMR discussions, Dr Mick Cooper at the University of Nottingham for mass spectrometry and Mr Stephen Boyer (London Metropolitan University) for elemental analyses.

Keywords: hydrophosphination • iron • isocyanates • *m*-terphenyl ligands • homogeneous catalysis

References

[1] a) D. W. Allen, *Organophosphorus Chem* **2016**, *45*, 1–50; b) D. E. C. Corbridge, *Phosphorus: Chemistry, Biochemistry and Technology*, 6th ed., CRC Press, Boca Raton, FL, **2013**.

[2] a) I. Wauters, W. Debrouwer, C. V. Stevens, *Beilstein J. Org. Chem.* **2014**, *10*, 1064–1096; b) S. Greenberg, D. W. Stephan, *Chem. Soc. Rev.* **2008**, *37*, 1482–1489.

[3] a) C. A. Bange, R. Waterman, *Chem. Eur. J.* **2016**, *22*, 12598–12605; b) V. Koshti, S. Gaikwad, S. H. Chikkali, *Coord. Chem. Rev.* **2014**, *265*, 52–73; c) L. Rosenberg, *ACS Catal.* **2013**, *3*, 2845–2855.

[4] For selected references: a) M. Espinal-Viguri, A. K. King, J. P. Lowe, M. F. Mahon, R. L. Webster, *ACS Catal.* **2016**, *6*, 7892–7897; b) M. Itazaki, S. Katsube, M. Kamitani, H. Nakazawa, *Chem. Commun.* **2016**, *52*, 3163–3166; c) A. Di Giuseppe, R. De Luca, R. Castarlenas, J. J. Perez-Torrente, M. Crucianelli, L. A. Oro, *Chem. Commun.* **2016**, *52*, 5554–5557; d) C. A. Bange, R. Waterman, *ACS Catal.* **2016**, *6*, 6413–6416; e) L. Routaboul, F. Toulgoat, J. Gatignol, J. F. Lohier, B. Norah, O. Delacroix, C. Alayrac, M. Taillefer, A. C. Gaumont, *Chem. Eur. J.* **2013**, *19*, 8760–8764; f) A. M. Geer, A. L. Serrano, B. de Bruin, M. A. Ciriano, C. Tejel, *Angew. Chem. Int. Ed. Engl.* **2015**, *54*, 472–475; *Angew. Chem*. **2015**, *127*, 482–485; g) P. E. Sues, A. J. Lough, R. H. Morris, *J. Am. Chem. Soc.* **2014**, *136*, 4746–4760.

[5] a) R. J. Batrice, M. S. Eisen, *Chem. Sci.* **2016**, *7*, 939–944; b) I. S. Karmel, M. Tamm, M. S. Eisen, *Angew. Chem. Int. Ed.* **2015**, *54*, 12422–12425; *Angew. Chem*. **2015**, *127*, 12599–12602; c) X. Gu, L. Zhang, X. Zhu, S. Wang, S. Zhou, Y. Wei, G. Zhang, X. Mu, Z. Huang, D. Hong, F. Zhang, *Organometallics* **2015**, *34*, 4553–4559; d) W. Ma, L. Xu, W.-X. Zhang, Z. Xi, *New J. Chem.* **2015**, *39*, 7649–7655; e) A. C. Behrle, J. A. R. Schmidt, *Organometallics* **2013**, *32*, 1141–1149; f) W. X. Zhang, Z. Hou, *Org. Biomol. Chem.* **2008**, *6*, 1720–1730; g) W. X. Zhang, M. Nishiura, T. Mashiko, Z. Hou, *Chem. Eur. J.* **2008**, *14*, 2167–2179.

[6] W. X. Zhang, M. Nishiura, Z. Hou, *Chem. Commun.* **2006**, 3812–3814.

[7] a) M. De Tullio, A. Hernan-Gomez, Z. Livingstone, W. Clegg, A. R. Kennedy, R. W. Harrington, A. Antinolo, A. Martinez, F. Carrillo-Hermosilla, E. Hevia, *Chem. Eur. J.* **2016**, *22*, 17646–17656; b) Mark R. Crimmin, Anthony G. M. Barrett, Michael S. Hill, Peter B. Hitchcock, P. A. Procopiou, *Organometallics* **2008**, *27*, 497–499.

[8] D. L. Kays, A. R. Cowley, *Chem. Commun.* **2007**, *10*, 1053–1055.

[9] H. R. Sharpe, A. M. Geer, H. E. Williams, T. J. Blundell, W. Lewis, A. J. Blake, D. L. Kays, *Chem. Commun.* **2017**, *53*, 937–940.

[10] Y. Sun, Z. Zhang, X. Wang, X. Li, L. Weng, X. Zhou, *Dalton Trans.* **2010**, 221–226.

[11] a) A. R. Jupp, G. Trott, É. P. de la Garanderie, J. D. Holl, D. Carmichael, J. M. Goicoechea, *Chem. Eur. J.* **2015**, *21*, 8015–8018; b) A. R. Jupp, J. M. Goicoechea, *J. Am. Chem. Soc.* **2013**, *135*, 19131–19134; c) P. Štěpnička, *Chem. Soc. Rev.* **2012**, *41*, 4273–4305.

[12] a) D. T. Seidenkranz, J. M. McGrath, L. N. Zakharov, M. D. Pluth, *Chem. Commun.* **2017**, *53*, 561–564; b) P. W. Miller, M. Nieuwenhuyzen, J. P. H. Charmant, S. L. James, *Inorg. Chem.* **2008**, *47*, 8367–8379.

[13] a) L. Melendez-Alafort, A. Nadali, G. Pasut, E. Zangoni, R. De Caro, L. Cariolato, M. C. Giron, I. Castagliuolo, F. M. Veronese, U. Mazzi, *Nucl. Med. Biol.* **2009**, *36*, 57–64; b) C. Fernandes, J. D. G. Correia, L. Gano, I. Santos, S. Seifert, R. Syhre, R. Bergmann, H. Spies, *Bioconjugate Chem.* **2005**, *16*, 660–668; c) T. Kniess, J. D. G. Correia, A. Domingos, E. Palma, I. Santos, *Inorg. Chem.* **2003**, *42*, 6130–6135.

[14] a) F. Sladojevich, A. Trabocchi, A. Guarna, D. J. Dixon, *J. Am. Chem. Soc.* **2011**, *133*, 1710–1713; b) M. Léautey, P. Jubault, X. Pannecoucke, J.-C. Quirion, *Eur. J. Org. Chem.* **2003**, *2003*, 3761–3768.

[15] a) R. H. Crabtree, *Chem. Rev.* **2012**, *112*, 1536–1554; b) J. A. Widegren, R. G. Finke, *J. Mol. Catal. A: Chem.* **2003**, *198*, 317–341.

[16] K. J. Gallagher, R. L. Webster, *Chem. Commun.* **2014**, *50*, 12109–12111.

[17] a) C. Scriban, D. S. Glueck, L. N. Zakharov, L. N. Kassel, A. G. DiPasquale, J. A. Golen, A. L. Rheingold, *Organometallics* **2006**, *25*, 5757–5767; b) C. Scriban, I. Kovacik, D. S. Glueck, *Organometallics* **2005**, *24*, 4871–4874.

[18] M. D. Greenhalgh, A. S. Jones, S. P. Thomas, *ChemCatChem* **2015**, *7*, 190–222.

[19] a) A. D. Sadow, A. Togni, *J. Am. Chem. Soc.* **2005**, *127*, 17012–17024; b) F. Jérôme, F. Monnier, H. Lawicka, S. Dérien, P. H. Dixneuf, *Chem. Commun.* **2003**, 696–697; c) M. A. Kazankova, M. O. Shulyupin, I. P. Beletskaya, *Synlett* **2003**, *2003*, 2155–2158.

[20] a) B. M. Cochran, F. E. Michael, *J. Am. Chem. Soc.* **2008**, *130*, 2786–2792; b) M. R. Douglass, C. L. Stern, T. J. Marks, *J. Am. Chem. Soc.* **2001**, *123*, 10221–10238.

Supplementary Information

General Procedures

All compounds prepared herein are air and moisture sensitive; therefore, all reactions and manipulations were performed by using standard Schlenk line and glovebox equipment under an atmosphere of purified argon or nitrogen. *Iso*-hexane (contains <5% *n*-hexane) and *n*-pentane were dried by passing through a column of activated 4 Å molecular sieves. THF and toluene were freshly distilled over sodium benzophenone ketyl (THF) or molten potassium (toluene) under nitrogen. All solvents were degassed *in vacuo* and stored over a potassium mirror (*iso*-hexane, *n*-pentane, toluene) or activated 4 Å molecular sieves (THF) prior to use. Benzene-d_6 was dried over potassium, and THF-d_8 was dried over CaH_2. Both were degassed with three freeze/pump/thaw cycles prior to use. NMR spectroscopy were performed on either a Bruker DPX400, AV400, AV(III)400, AV(III)400HD, AV(III)500, AV(III)600 or AV(III)800 spectrometers. Chemical shifts are quoted in ppm relative to neat TMS (^{1}H, $^{13}C\{^{1}H\}$), LiCl/D_2O solution ($^{7}Li\{^{1}H\}$), H_3PO_4 ($^{31}P\{^{1}H\}$), $MeNO_2$ (^{15}N). Selected ^{15}N NMR resonances were obtained from ^{1}H, ^{15}N HSQC. $[2,6\text{-}Tmp_2C_6H_3Li]_2$,[1] $(2,6\text{-}Tmp_2C_6H_3)_2Fe(THF)$[1] and $(2,6\text{-}Mes_2C_6H_3)_2Fe$[2] were prepared following the procedures described in the literature. Mass spectra were measured by the departmental service at the University of Nottingham. IR absorption spectroscopy were recorded on a Bruker Alpha FTIR instrument with a 'Platinum' ATR attachment. Elemental microanalysis was performed by Mr Stephen Boyer at the Microanalysis Service, London Metropolitan University, UK. All the isocyanates are commercially available and were transferred directly into the glovebox after which 4 Å molecular sieves were added with the exception of 3,5-dimethoxyphenyl isocyanate which was dried overnight under vacuum. Diphenylphosphine (Sigma-Aldrich) was supplied in a Sure/Seal™ bottle and was transferred directly into the glove box.

Table S1. Catalytic hydrophosphination of isocyanates mediated by complex **1** in THF.[a]

Entry	RNCO	RNCO: Ph2PH	T (ºC)	t(h)	Cat.	Conv. (%)[b]	**3/4/5** (%)[c]
1	Ph	1:1	25	16	**1**	40	97/0/3
2	Ph	1:1	60	32	**1**	80	100/0/0
3	$(OMe)_2C_6H_3$	1:1	60	32	**1**	66	99/1/0
4	$4\text{-}BrC_6H_4$	1:1	60	24	**1**	50	98/0/2

[a] Reaction conditions: 0.6 mL of THF, 5 mol% cat. [b] Determined by $^{31}P\{^1H\}$ NMR spectroscopy. [c] Ratio determined by $^{31}P\{^1H\}$ NMR.

Table S2. Catalytic hydrophosphination of isocyanates mediated by complex **1** with additives.[a]

Entry	RNCO	RNCO: Ph2PH	t(h)	Additive	Cat.	Conv. (%)[b]	**3/4/5** (%)[c]
1	$3,5\text{-}(OMe)_2C_6H_3$	2:1	16	NEt_3	**1**	>99	37/63/0
2	$3,5\text{-}(OMe)_2C_6H_3$	2:1	16	$NEt_3{\cdot}HCl$[d]	**1**	>99	3/97/0
3	$3,5\text{-}(OMe)_2C_6H_3$	2:1	16	$NEt_3{\cdot}HCl$[d]	- [e]	19	94/0/1[f]
4	Ph	2:1	16	$NEt_3{\cdot}HCl$[d]	**1**	>99	1/99/0
5	Cy	1:1	48	$NEt_3{\cdot}HCl$[d]	**1**	0	-

[a] Reaction conditions: 25 ºC, 0.6 mL of C_6D_6, 5 mol% cat. [b] Determined by ^1H NMR and $^{31}P\{^1H\}$ NMR spectroscopy. [c] Ratio determined by ^1H NMR and $^{31}P\{^1H\}$ NMR. [d] 0.5 eq. wrt Ph_2PH; several drops of THF-d_8 are added to solubilise $NEt_3{\cdot}HCl$. [e] Reactions performed without catalyst. [f] 5% unidentified $^{31}P\{^1H\}$ NMR peak.

Table S3. Selected Data for **3a, c**-**h** and **4a**-**e**,**i**.

	Isolated Yield (%)	^{31}P (ppm)	$^{13}C_{PCO}$ (ppm)	$^{1}J(C,P)$ (Hz)	$^{1}H_{NH}$ (ppm)	$^{15}N_{NH}$ (ppm)	ν_{PCO} (cm^{-1})	ν_{NCONH} (cm^{-1})
3a	71	–0.2	175.2	15	7.24	-	1688[a]	-
3c	57	0.8	175.5	16	7.37	-	1630	-
3d	64	0.2	175.4	16[a]	7.00	-	1630[a]	-
3f	56	–4.3	174.9	12	5.44	111.2	1645	-
3g	57	–4.0	175.0	13	5.35	113.5	1641	-
3h	67	–2.7	175.3	13	5.42	117.6	1632	-
4a	50	8.3	184.9	29	11.57	116.7	1718	1588
4b	55	8.0	184.9	28	11.58	-	1716	1536
4c	65	7.7	184.9	30	11.74	-	1719	1544
4d	79	8.8	185.0	31	11.41	-	1717	1594
4e	-	8.4	182.8	25	9.22	-	-	-
4i	-	7.8	183.6	27	9.22	-	-	-

[a] values from reference 3

General Procedures for the Catalytic Hydrophosphination of Isocyanates

Standard procedure for the catalytic hydrophosphination of isocyanates: In a Young's NMR tube 5 mol% of the precatalyst (**1**: 10.0 mg, 0.0147 mmol; **2**: 10.0 mg, 0.0132 mmol) was dissolved in C_6D_6 (0.6 mL) in a glove-box with the corresponding isocyanate and Ph_2PH (1:1 or 2:1 of RNCO:Ph_2PH). The reaction was either carried out at room temperature and monitored by ^1H and $^{31}P\{^1H\}$ NMR spectroscopy or heated to 60 °C; the samples were maintained at 60 °C for 16 h and ^1H and $^{31}P\{^1H\}$ NMR spectroscopy were performed at the final time. Conversion was quantified by integration of ^1H and $^{31}P\{^1H\}$ NMR spectra.

Standard procedure for *in situ* NMR reaction monitoring for the catalytic hydrophosphination of isocyanates: In a Young's NMR tube 5 mol% of precatalyst (**1**: 10.0 mg, 0.0147 mmol; **2**: 10.0 mg, 0.0132 mmol) was dissolved in C_6D_6 (0.6 mL) with the corresponding isocyanate. The solution was cooled to –30 °C after which Ph_2PH (1:1 or 2:1 of RNCO:Ph_2PH) was added and the sample cooled to –78 °C to prevent the reaction from initiating. The sample was then transferred to the NMR spectrometer and monitored directly at 25 °C or heated to 60 °C. Conversion was quantified by integration of ^1H and $^{31}P\{^1H\}$ NMR spectra.

Standard procedure for the catalytic hydrophosphination of isocyanates in THF: In a Young's NMR tube 5 mol% of the precatalyst (**1**: 10.0 mg, 0.0147 mmol) was dissolved in THF (0.6 mL) in a glove-box with the corresponding isocyanate (0.293 mmol), Ph_2PH (51 µL, 0.293 mmol) and a C_6D_6 insert. The reaction was either carried out at room temperature or heated to 60 °C and monitored by $^{31}P\{^1H\}$ NMR spectroscopy. Conversion was quantified by integration of the $^{31}P\{^1H\}$ NMR spectrum.

Catalytic hydrophosphination of Isocyanates with Additives

***In situ* NMR reaction monitoring for the catalytic hydrophosphination of isocyanates with additives:** In a Young's NMR tube 5 mol% of the precatalyst **1** (10.0 mg, 0.0147 mmol) was dissolved in C_6D_6 (0.6 mL) with CyNCO (38 µL, 0.294 mmol) and the corresponding additive (see Table S4 below). The solution was cooled to –30 °C after which Ph_2PH (51 µL, 0.294 mmol) was added and the sample cooled to –78 °C to prevent the reaction from initiating. The sample was then transferred to the NMR spectrometer and monitored directly at 25 °C. Conversion was quantified by integration of ^1H and $^{31}P\{^1H\}$ NMR spectra.

Table S4. Additives and quantities used in the *in situ* NMR reaction monitoring experiments.

Additive	
CS_2 (0.05 M in toluene)	29 µL, 0.00147 mmol
Hg (l)	*ca.* 1 drop
Cumene	10 µL, 0.0735 mmol

Catalytic hydrophosphination of isocyanates with weak base/acid: In a Young's NMR tube 5 mol% of the precatalyst **1** (10.0 mg, 0.0147 mmol), the corresponding isocyanate, Ph_2PH (51 µL, 0.294 mmol) and the additive (see Table S5 below) were dissolved in C_6D_6 (0.6 mL) in a glove-box. The reactions were kept at room temperature and monitored by ^1H and $^{31}P\{^1H\}$ NMR at the final time. Conversion was quantified by integration of ^1H and $^{31}P\{^1H\}$ NMR spectra.

Table S5. Additives and isocyanate quantities used in the catalytic hydrophosphination of isocyanates with a weak base (NEt_3) or weak acid ($Et_3N{\cdot}HCl$).

Additive	**RNCO**		**Solvent**	**Time**
NEt_3 (41 µL, 0.294 mmol)	3,5-$(OMe)_2$ C_6H_3	(105 mg, 0.588 mmol)	C_6D_6 (0.6 mL)	16 h
$Et_3N{\cdot}HCl$ (40.4 mg, 0.294 mmol)	3,5-$(OMe)_2$ C_6H_3	(105 mg, 0.588 mmol)	C_6D_6 (0.6 mL), THF-d_8 (*ca.* 2 drops)	16 h
	Ph	(64 µL, 0.588 mmol)	C_6D_6 (0.6 mL), THF-d_8 (*ca.* 2 drops)	16 h
	Cy	(75 µL, 0.588 mmol)	C_6D_6 (0.6 mL), THF-d_8 (*ca.* 2 drops)	48 h

Catalytic hydrophosphination of Isocyanates with Mixed Isocyanates

Hydrophosphination with PhNCO and CyNCO:

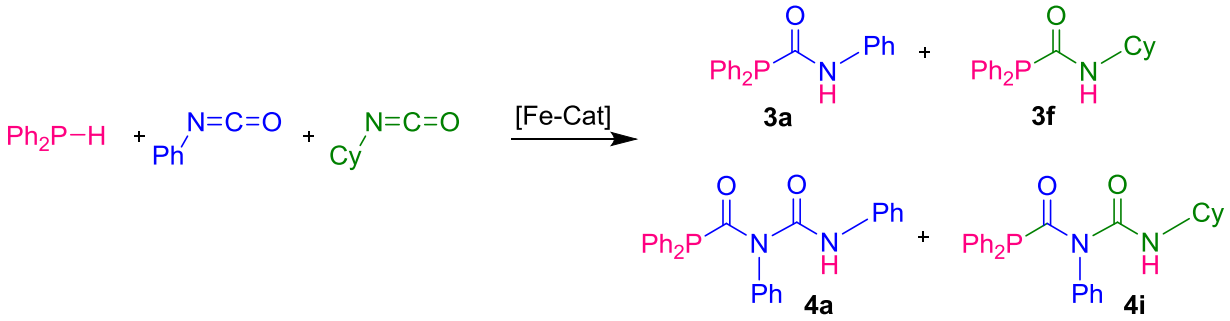

Scheme S1. Hydrophosphination of mixture of phenyl and cyclohexyl isocyanate with diphenylphosphine (1:1:1) using **1**. A combination of 4 products are obtained **3a**/**3f**/**4a**/**4i**.

Experimental procedure: In a Young's NMR tube 5 mol% of the precatalyst (**1**: 10.0 mg, 0.0147 mmol) was dissolved in C_6D_6 (0.6 mL) in a glove-box with Ph_2PH (51 µL, 0.293 mmol), PhNCO (32 µL, 0.293 mmol) and CyNCO (37 µL, 0.293 mmol). The reaction was carried out at room temperature and monitored by ^1H and $^{31}P\{^1H\}$ NMR spectroscopy. After 16 h at room temperature catalysis was complete (>99% conversion) and the formation of **3a**, **3f**, **4a** and **4i** were observed by NMR with a ratio of 26:27:30:17 (**3a**:**3f**:**4a**:**4i**). Selected spectroscopic data for phosphacarboxamide **4i**: ^1H NMR (400 MHz, C_6D_6, 25 ºC) δ = 9.22 (s, 1H, N*H*), 7.63–6.82 (Ar), 3.93 (CH_2), 1.97–1.87 (m, CH_2), 1.49–1.45 (m, CH_2), 1.18 (m, CH_2), 1.11–1.04 (m, CH_2). $^{31}P\{^1H\}$ NMR (162 MHz, C_6D_6, 25 ºC) δ = 7.8 (s, 1P, Ph_2P). MS (ESI) Expected: 431.1883, found: 431.1883 $[M+H]^+$ (err [ppm] = 0.1).

Procedures for the Scaled-up Catalytic Hydrophosphination of Isocyanates

3a, c and d: In a Schlenk flask 5 mol% of **1** (30.0 mg, 0.0441 mmol), Ph_2PH (153 µL, 0.880 mmol) and the isocyanate (0.880 mmol) were dissolved in THF (1.5 mL) and stirred at 60 °C for 3 days (**3a** and **3c**) or 2 days (**3d**). The solvent was removed *in vacuo* and the solid was washed with cold *iso*-hexane (3 × 5 mL) and dried under vacuum resulting in the isolation of the corresponding pure phosphinocarboxamide as a white powder (**3a**: 190 mg, 71%; **3c**: 184 mg, 57%; **3d**: 217 mg, 64%).

3f-h: In a Schlenk flask 5 mol% of **1** (30.0 mg, 0.0441 mmol), Ph_2PH (153 µL, 0.880 mmol) and the isocyanate (0.880 mmol) were dissolved in toluene (5 mL) and stirred at room temperature (Cy) or at 60 °C (^{i}Pr, ^{t}Bu) for 16 h. The solvent was removed *in vacuo* and the oily residue was extracted into *n*-pentane (2 × 10 mL) and stored at –30 °C for one day. This resulted in the precipitation of while crystalline solid of the corresponding pure phosphinocarboxamide (**3f**: 153 mg, 56%; **3g**: 137 mg, 57%; **3h**: 168 mg, 67%).

4a-d: In a Schlenk flask 5 mol% of **1** (30.0 mg, 0.0441 mmol), Ph_2PH (153 µL, 0.880 mmol) and the isocyanate (1.76 mmol) were dissolved in toluene (5 mL) and stirred at room temperature for 16 h. The solvent was removed *in vacuo* and the oily residue was washed with *n*-pentane (2 × 10 mL) and dried for *ca.* 6 h enabling the isolation of the a while solid of the corresponding phosphinocarboxamide (**4a**: 186 mg, 50%; **4b**: 220 mg, 55%; **4c**: 304 mg, 65%, **4d**: 406 mg, 79%).

Large Scale-up: In a Schlenk flask 5 mol% of **1** (102 mg, 0.150 mmol), Ph_2PH (522 µL, 3.00 mmol), PhNCO (653 µL, 6.00 mmol) and $Et_3N{\cdot}HCl$ (404 mg, 2.93 mmol) were dissolved in toluene (6 mL) and stirred at room temperature for 16 h. The solvent was removed *in vacuo* and the product was extracted into toluene (20 mL) and the solvent removed yielding a white solid which was dried for *ca.* 3 h. The solid was washed with *iso*-hexane (3 × 10 mL) and dried for *ca.* 6 h enabling the isolation of the a while solid of the corresponding phosphinocarboxamide (**4a**: 936 mg, 74%).

Spectroscopic Data

$Ph_2PC(=O)NH(Ph)$ (3a).

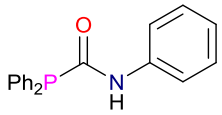

White solid: 190 mg, 71%.^{1}H NMR (400 MHz, C_6D_6, 25 ºC) δ 7.64–7.52 (m, 4H, PPh_2^o), 7.35 (d, ^3J(H,H) = 8.0 Hz, 2H, Ph^o), 7.24 (d, ^3J(H,P) = 7.6 Hz, 1H, N*H*), 7.07–7.01 (m, 6H, PPh_2^{m+p}), 6.98 (t, ^3J(H,H) = 7.9 Hz, 2H, Ph^m), 6.82 (t, ^3J(H,H) = 7.4 Hz, 1H, Ph^p). $^{13}C\{^1H\}$ NMR (101 MHz, C_6D_6, 25 ºC) δ = 175.2 (d, ^1J(C,P) = 15 Hz, *C*=O), 138.5 (Ph^i), 134.8 (d, ^2J(C,P) =19 Hz, PPh_2^o), 134.3 (d, ^1J(C,P) = 10 Hz, PPh_2^i), 129.9 (PPh_2^m), 129.3 (Ph^m), 129.2 (PPh_2^p), 124.6 (Ph^p), 119.4 (Ph^o). $^{31}P\{^1H\}$ (162 MHz, C_6D_6, 25 ºC) δ –0.2 (s, 1P, Ph_2P). MS (ESI) Expected: 306.1039, found: 306.1042 (err [ppm] = 1.00) $[M+H]^+$ (100%). Spectroscopic data matched previous reported literature.[3]

$Ph_2PC(=O)NH[3,5\text{-}(OMe)_2C_6H_3]$ (3c).

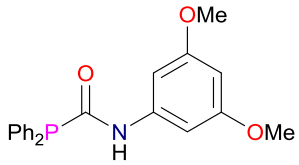

White solid: 184 mg, 57%.^{1}H NMR (400 MHz, C_6D_6, 25 ºC) δ = 7.57 (td, ^3J(H,H) = 6.9, ^3J(H,P) = 6.9, ^4J(H,H) = 2.9 Hz, 4H, PPh_2^o), 7.37 (s, 1H, N*H*), 7.18–6.94 (m, 6H, PPh_2^{m+p}), 6.91–6.75 (m, 2H, Ph^o), 6.34 (s, 1H, Ph^p), 3.27 (s, 6H, O*C*H_3). $^{13}C\{^1H\}$ NMR (101 MHz, C_6D_6, 25 ºC) δ 175.5 (d, ^1J(C,P) = 16 Hz, *C*=O), 161.8 (Ph^m), 140.4 (d, ^3J(C,P) = 5 Hz, Ph^i), 134.7 (d, ^1J(C,P) = 19 Hz, PPh^i,), 134.2 (d, ^2J(C,P) = 11 Hz, PPh_2^o), 129.9 (PPh_2^p), 129.2 (d, ^3J(C,P) = 7 Hz, PPh_2^m), 97.9 (Ph^o), 97.6 (Ph^p), 55.0 (O*C*H_3). $^{31}P\{^1H\}$ (162 MHz, C_6D_6, 25 ºC) δ 0.8 (s, 1P, Ph_2P). MS (ESI) Expected: 366.1257, found: 366.1254 (err [ppm] = 1.00) $[M+H]^+$ (100%). IR (ATR) ν/cm^{-1} = 3278 (N-H), 1630 (C=O).

$Ph_2PC(=O)NH(4\text{-}BrC_6H_4)$ (3d).

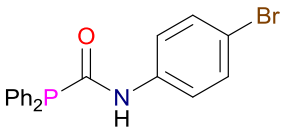

White solid: 217 mg, 64%.^{1}H NMR (400 MHz, C_6D_6, 25 ºC) δ 7.62–7.45 (m, 4H, PPh_2^o), 7.09–7.01 (m, 9H, N*H*, PPh_2^{m+p}, Ph^o), 6.96 (d, ^3J(H,H) = 8.6 Hz, 2H, Ph^m). $^{13}C\{^1H\}$ NMR (151 MHz, C_6D_6, 25 ºC) δ 175.4 (d, ^1J(C,P) = 16 Hz, *C*=O), 137.3 (Ph^i), 134.8 (d, ^2J(C,P) = 19 Hz, PPh_2^o), 134.0 (d, ^1J(C,P) = 10 Hz, PPh^i), 132.1 (Ph^o), 130.0 (PPh^p), 129.2 (d, ^3J(C,P) = 5 Hz PPh^m), 121.1 (Ph^m), 117.1 (Ph^p). $^{31}P\{^1H\}$ (162 MHz, C_6D_6, 25 ºC) δ 0.2 (s, 1P, Ph_2P). MS (ESI) Expected: 405.9967, found: 405.9966 (err [ppm] = 0.10) $[M+Na]^+$ (100%). Spectroscopic data matched previous reported literature.[3]

$Ph_2PC(=O)NH(Cy)$ (3f).

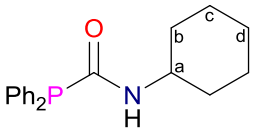

White solid: 153 mg, 56%. ^{1}H NMR (800 MHz, C_6D_6, 25 ºC) δ 7.67 (td, ^3J(H,H) = 7.4 Hz, ^3J(H,P) = 7.4 Hz, ^4J(H,H) = 1.4 Hz, 4H, PPh_2^o), 7.12–7.02 (m, 6H PPh_2^{m+p}), 5.44 (br d, ^3J(H,P) = 4.1 Hz, 1H, N*H*), 3.95 (dddd, *J* = 14.2, 10.2, 7.8, 3.9 Hz, 1H, CH^a), 1.63 (dt, ^2J(H,H) = 12.9 Hz, ^3J(H,H) = 4.3 Hz, 2H, CH^b), 1.27 (dt, ^2J(H,H) = 13.7, ^2J(H,H) = 4.2 Hz, 2H, CH^c), 1.23 (dt, ^2J(H,H) = 12.8 Hz, ^2J(H,H) = 4.2 Hz, 1H, C$H^{d'}$), 1.07–0.98 (m, 2H, C$H^{c'}$), 0.79 (ddt, ^2J(H,H) = 11.6 Hz, ^2J(H,H) = 11.6 Hz, 3.6, 1H, C$H^{d''}$), 0.74–0.65 (m, 2H, C$H^{b'}$). ^{13}C{^{1}H} NMR (101 MHz, C_6D_6, 25 ºC) δ 174.9 (d, ^1J(C,P) = 12 Hz, *C*O), 135.4 (d, ^1J(C,P) = 12 Hz, PPh_2^i), 134.7 (d, ^2J(C,P) = 19 Hz, PPh_2^o), 129.6 (PPh_2^p), 129.0 (d, ^3J(C,P) = 6.6 Hz, PPh_2^m), 48.7 (*C*H), 32.8 (C^bH_2), 25.6 (C^dH_2), 24.7 (C^cH_2). ^{31}P{^{1}H} (162 MHz, C_6D_6, 25 ºC) δ –4.3 (s, 1P, Ph_2P). ^{15}N NMR (81 MHz, C_6D_6, 25 ºC) δ 111.2 (1N, *N*H). MS (ESI) Expected: 312.1512, found: 312.1526 (err [ppm] = 4.60) $[M+H]^+$ (100%). Elemental analysis $C_{19}H_{22}NOP$: calcd. C 73.29, H 7.12, N 4.50; found: C 73.16, H 7.00, N 4.58 %. IR (ATR) *v*/cm^{-1} = 3244 (N-H), 1645 (C=O). Spectroscopic data matched previous reported literature.[3]

$Ph_2PC(=O)NH(^iPr)$ (3g).

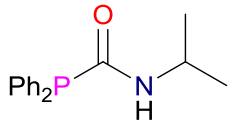

White crystalline solid: 137 mg, 57%. ^{1}H NMR (800 MHz, C_6D_6, 25 ºC) δ 7.64 (ddd, ^3J(H,H) = 7.5 Hz, ^3J(H,P) = 7.5 Hz, ^4J(H,P) = 1.5 Hz, 4H PPh_2^o), 7.07 (t, ^3J(H,H) = 7.4 Hz, 4H PPh_2^m), 7.06–7.03 (m, 2H, PPh_2^p), 5.35 (s, 1H, N*H*), 4.14 (oct, ^3J(H,H) = 6.8 Hz, 1H, C*H*), 0.72 (d, ^3J(H,H) = 6.6 Hz, 6H, CH_3). ^{13}C{^{1}H} (101 MHz, C_6D_6, 25 ºC) δ 175.0 (d, ^1J(C,P) = 13 Hz, *C*O), 135.2 (d, ^1J(C,P) = 12 Hz, PPh_2^i), 134.6 (d, ^2J(C,P) = 19 Hz, PPh_2^o), 129.6 (s, PPh_2^p), 129.0 (d, ^3J(C,P) = 7 Hz, PPh_2^m), 42.1 (*C*H), 22.3 (CH_3). ^{31}P{^{1}H} (162 MHz, C_6D_6, 25 ºC) δ –4.0 (s, 1P, Ph_2P). ^{15}N NMR (81 MHz, C_6D_6, 25 ºC) δ 113.5 (1N, *N*H). MS (ESI) Expected: 272.1199, found: 272.1205 (err [ppm] = 2.40) $[M+H]^+$ (62.1 %). IR (ATR) *v*/cm^{-1} = 3258 (N-H), 1641 (C=O).

$Ph_2PC(=O)NH(^tBu)$ (3h).

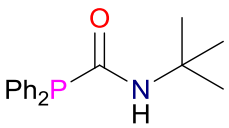

White crystalline solid: 168 mg, 67%. ^{1}H NMR (800 MHz, C_6D_6, 25 ºC) δ 7.64 (ddd, ^3J(H,H) = 7.5 Hz, ^3J(H,P) = 7.5 Hz, ^3J(H,P) = 1.7 Hz, 4H, PPh_2^o), 7.07 (t, ^3J(H,H) = 7.4 Hz, 4H PPh_2^m), 7.05–7.02 (m, 2H, PPh_2^p), 5.42 (s, 1H, N*H*), 1.12 (s, 9H, CH_3). ^{13}C{^{1}H} (101 MHz, C_6D_6, 25 ºC) δ 175.3 (d, ^1J(C,P) = 13 Hz, *C*O), 135.6 (d, ^1J(C,P) = 12 Hz, PPh_2^i), 134.6 (d, ^2J(C,P) = 19 Hz, PPh_2^o), 129.5 (s, PPh_2^p), 129.0 (d, ^3J(C,P) = 7 Hz, PPh_2^m), 52.5 (d, ^3J(C,P) = 3 Hz, $(C(CH_3)_3)$, 28.6 (CH_3).

$^{31}P\{^{1}H\}$ (162 MHz, C_6D_6, 25 ºC) δ –2.7 (s, 1P, Ph_2P). ^{15}N NMR (81 MHz, C_6D_6, 25 ºC) δ 117.6 (1N, *N*H). MS (ESI) Expected: 286.1355, found: 286.1372 (err [ppm] = 5.90) $[M+H]^+$ (72.2 %). Elemental analysis $C_{17}H_{20}NOP$: calcd. C 71.56, H 7.07, N 4.91; found: C 71.63 H 6.93, N 5.01 %. IR (ATR) *v*/cm^{-1} = 3310 (N-H), 1632 (C=O).

$Ph_2PC(=O)N(Ph)C(=O)NH(Ph)$ (4a).

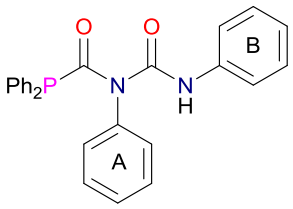

White solid: 186 mg, 50%. ^{1}H NMR (800 MHz, C_6D_6, 25 ºC) δ = 11.57 (s, 1H, N*H*), 7.67 (d, ^{3}J(H,P) = 7.9 Hz, 2H, Ph^{Bo}), 7.31 (t, ^{3}J(H,P) = 7.8 Hz, ^{3}J(H,H) = 7.8 Hz, 4H, PPh^{o}), 7.13–6.97 (m, 8H, PPh_2^{m+p} + Ph^{Bm}), 6.92 (t, ^{3}J(H,H) = 7.3 Hz, 1H, Ph^{Ap}), 6.87–6.82 (m, 3H, Ph^{Bp} + Ph^{Am}), 6.80 (d, ^{3}J(H,H) = 7.9 Hz, 2H, Ph^{Ao}). $^{13}C\{^{1}H\}$ (101 MHz, C_6D_6, 25 ºC) δ 184.9 (d, ^{1}J(C,P) = 29 Hz, P*C*=O), 151.2 (*C*=O), 138.7 (Ph^{Bi}), 136.5 (d, ^{3}J(C,P) = 4 Hz, Ph^{Ai}), 135.1 (d, ^{2}J(C,P) = 21 Hz, PPh_2^{o}), 133.3 (d, ^{1}J(C,P) = 8 Hz, PPh_2^{i}), 132.3 (d, ^{4}J(C,P) = 4 Hz, Ph^{Ao}), 129.9 (PPh_2^{p}), 129.4 (Ph^{Bm}), 129.2 (Ph^{Ap}), 128.8 (PPh_2^{m}), 128.7 (Ph^{Am}), 124.2 (Ph^{Bp}), 120.1 (Ph^{Bo}). $^{31}P\{^{1}H\}$ (162 MHz, C_6D_6, 25 ºC) 8.3 (s, 1P, Ph_2P). ^{15}N NMR (81 MHz, C_6D_6, 25 ºC) δ 116.7 (1N, *N*H). MS (ESI) Expected: 425.1413, found: 425.1414 (err [ppm] = 0.10) $[M+H]^+$ (30.6 %). IR (ATR) *v*/cm^{-1} = 3259 (N-H), 1718 (PC=O), 1588 (C=O).

$Ph_2PC(=O)N(^{p}Tol)C(=O)NH(^{p}Tol)$ (4b).

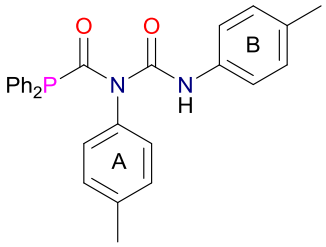

White solid: 220 mg, 55%. ^{1}H NMR (400 MHz, C_6D_6, 25 ºC) δ 11.58 (s, 1H, N*H*), 7.63 (d, ^{3}J(H,H) = 8.2 Hz, 2H, Ph^{Bo}), 7.35 (td, ^{3}J(H,H) = 8.1, ^{3}J(H,P) = 8.1, ^{4}J(H,H) =1.6 Hz, 4H, PPh_2^{o}), 7.06–6.98 (m, 6H, PPh_2^{m+p}), 6.88 (d, ^{3}J(H,H) = 8.2 Hz, 2H, Ph^{Bm}), 6.73 (dd,^{3}J(H,H) = 8.1 Hz, ^{5}J(H,P) = 1.5 Hz, 2H, Ph^{Ao}), 6.67 (d, ^{3}J(H,H) = 8.1 Hz, 2H, Ph^{Am}), 2.02 (s, 3H, CH_3^{B}), 1.97 (s, 3H, CH_3^{A}). $^{13}C\{^{1}H\}$ (101 MHz, C_6D_6, 25 ºC) δ 184.9 (d, ^{1}J(C,P) = 28 Hz, P*C*=O), 151.3 (*C*=O), 138.8 (Ph^{Ap}), 136.3 (Ph^{Bp}), 135.1 (d, ^{2}J(C,P) = 21 Hz, PPh_2^{o}), 134.0 (Ph^{Ai}), 133.6 (d, ^{1}J(C,P) = 8 Hz, PPh_2^{i}), 133.4 (Ph^{Bi}), 132.1 (d, ^{4}J(C,P) = 3 Hz, Ph^{Ao}), 130.0 (Ph^{Bm}), 129.2 (PPh_2^{p}), 129.1 (Ph^{Ao}), 128.7 (d, ^{3}J(C,P) = 8 Hz, PPh_2^{m}), 120.2 (Ph^{Bo}), 21.1 (CH_3^{A}), 20.8 (CH_3^{B}). $^{31}P\{^{1}H\}$ (162 MHz, C_6D_6, 25 ºC) δ 8.0 (s, 1P, Ph_2P). MS (ESI) Expected: 453.1726, found: 453.1731(err [ppm] = 1.10 $[M+H]^+$ (100 %). Elemental analysis $C_{28}H_{25}N_2O_2P$: calcd. C 74.32, H 5.57, N 6.19; found: C 74.01, H 5.39, N 6.07 %. IR (ATR) *v*/cm^{-1} = 3202 (N-H), 1716 (PC=O), 1536 (C=O).

$Ph_2PC(=O)N(3,5\text{-}(OMe)_2C_6H_3)C(=O)NH(3,5\text{-}(OMe)_2C_6H_3)$ (4c).

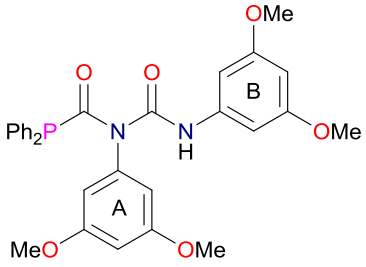

White solid: 304 mg, 65%.^{1}H NMR (400 MHz, C_6D_6, 25 ºC) δ 11.74 (s, 1H, N*H*), 7.43–7.34 (m, 4H, PPh_2^o), 7.22 (d, ^4J(H,H) = 2.3 Hz, 2H, Ph^{Bo}), 7.06–6.96 (m, 6H, PPh_2^{m+p}), 6.53 (t, ^4J(H,H) = 2.3 Hz, 1H, Ph^{Ap}), 6.42 (t, ^4J(H,H) = 2.3 Hz, 1H, Ph^{Bp}), 6.19 (dd, ^4J(H,H) = 2.3 Hz, ^5J(H,P) = 1.3 Hz, 2H, Ph^{Ao}), 3.30 (s, 6H, OCH_3^B), 3.09 (s, 6H, OCH_3^A). $^{13}C\{^1H\}$ (101 MHz, C_6D_6, 25 ºC) δ = 184.9 (d, ^1J(C,P) = 30 Hz, P*C*=O), 162.0 (Ph^{Bm}), 160.9 (Ph^{Am}), 151.1 (*C*=O), 140.5 (Ph^{Bi}), 138.2 (d, ^3J(C,P) = 4 Hz, Ph^{Ai}), 135.1 (d, ^2J(C,P) = 21 Hz, PPh_2^o),133.8 (d, ^1J(C,P) = 9 Hz, PPh_2^i), 129.8 (PPh_2^p), 128.8 (d, ^3J(C,P) = 8 Hz, PPh_2^m), 110.4 (d, ^4J(C,P) = 4 Hz, Ph^{Ao}), 102.8 (Ph^{Ap}), 98.4 (Ph^{Bo}), 97.8 (Ph^{Bp}), 54.9 (OCH_3^B), 54.9 (OCH_3^A).$^{31}P\{^1H\}$ (162 MHz, C_6D_6, 25 ºC) δ 7.7 (s, 1P, Ph_2P). MS (ESI) Expected: 545.1836, found: 545.1822 $[M+H]^+$ (err [ppm] = 2.50). Elemental analysis $C_{30}H_{29}N_2O_6P$: calcd. C 66.17, H 5.37, N 5.14; found: C 65.89, H 5.25, N 5.07 %. IR (ATR) *v*/cm^{-1} = 3161 (N-H), 1719 (PC=O), 1544 (C=O).

$Ph_2PC(=O)N(4\text{-}BrC_6H_4)C(=O)NH(4\text{-}BrC_6H_4)$ (4d).

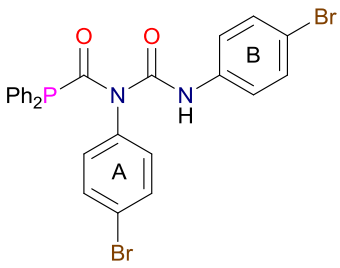

White solid: 406 mg, 79%.^{1}H NMR (400 MHz, C_6D_6, 25 ºC) δ 11.41 (s, 1H, N*H*), 7.58–7.47 (m, 4H, PPh_2^o), 7.30 (d, ^3J(H,H) = 9.0 Hz, 2H, Ph^{Bm}), 7.13 (d, ^3J(H,H) = 9.0 Hz, 2H, Ph^{Bo}), 7.09–6.97 (m, 6H, PPh_2^{m+p}), 6.92 (d, ^3J(H,H) = 8.6 Hz, 2H, Ph^{Am}), 6.40 (dd, ^3J(H,H) = 8.6 Hz, ^5J(H,P) = 1.5 Hz, 2H, Ph^{Ao}). $^{13}C\{^1H\}$ (101 MHz, C_6D_6, 25 ºC) δ 185.0 (d, ^1J(C,P) = 31 Hz, P*C*=O), 150.8 (*C*=O), 137.1 (Ph^{Bi}), 135.1 (d, ^2J(C,P) = 21 Hz, PPh_2^o), 134.7 (d, ^3J(C,P) = 4 Hz, Ph^{Ai}), 134.6 (Ph^{Ap}), 134.0 (PPh_2^i), 133.4 (d, ^4J(C,P) = 4 Hz, Ph^{Ao}), 132.1 (Ph^{Bo}), 131.3 (Ph^{Am}), 129.8 (PPh_2^p), 128.8 (d, ^3J(C,P) = 8 Hz, PPh_2^m), 121.3 (Ph^{Bm}), 116.6 (Ph^{Bp}). $^{31}P\{^1H\}$ (162 MHz, C_6D_6, 25 ºC) δ 8.8 (s, 1P, Ph_2P). MS (ESI) Expected: 580.9642, found: 580.9624 $[M+H]^+$ (err [ppm] = 3.20). IR (ATR) *v*/cm^{-1} = 3268 (N-H), 1717 (PC=O), 1594 (C=O).

$Ph_2PC(=O)N(^nHx)C(=O)NH(^nHx)$ (4e).

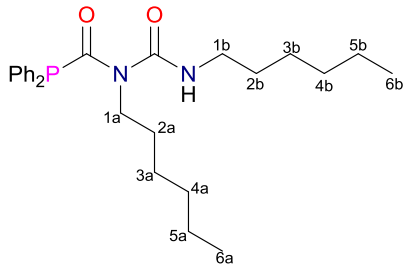

Was prepared *in situ* by addition of Ph_2PH (51 µL, 0.293 mmol) and ^nHxNCO (85 µL, 0.586 mmol) to a solution of **1** (10.0 mg, 5 mol%) in C_6D_6. After 16 h at r.t the solution was studied by NMR spectroscopy. Selected spectroscopic data: ^1H NMR (400 MHz, C_6D_6, 25 ºC) δ 9.22 (s, 1H, N*H*), 7.55–7.45 (m, 4H, PPh_2^o), 7.07-6.99 (m, 6H, PPh_2^{m+p}), 4.03 (t, 2H, ^3J(H,H) = 4.6 Hz, CH_2^{1a}), 3.25 (q, 2H, ^3J(H,H) = 4.2 Hz, CH_2^{1b}), 1.64 (m, 2H, CH_2^{2a}), 1.34 (br t, ^3J(H,H) = 5.6 Hz, CH_2^{2b}), 1.17–1.04 (m, 12H, $CH_2^{3a,4a,5a}$ + $CH_2^{3a,4a,5a}$), 0.81 (m, 4H, CH_3^{6a+6b}). $^{13}C\{^1H\}$ NMR (101 MHz, C_6D_6, 25 °C): δ 182.8 (d, ^1J(C,P) = 25 Hz, P*C*=O), 154.4 (*C*O), 135.0 (d, ^2J(C,P) = 20 Hz, PPh_2^o), 133.4 (d, ^1J(C,P) = 7 Hz, PPh_2^i), 46.2 (d, ^4J(C,P) = 19 Hz, CH_2^{1a}), 40.6 (CH_2^{1b}), 28.2 (CH_2^{2a+2b}), 26.6 (CH_2), 22.5 (CH_2), 14.4(CH_3^{6a+6b}). $^{31}P\{^1H\}$ (162 MHz, C_6D_6, 25 ºC) δ 8.4 (s, 1P, Ph_2P). MS (ESI) Expected: 441.2665, found: 441.2677 $[M+H]^+$ (err [ppm] = 2.60) (7.9%).

NMR Spectra

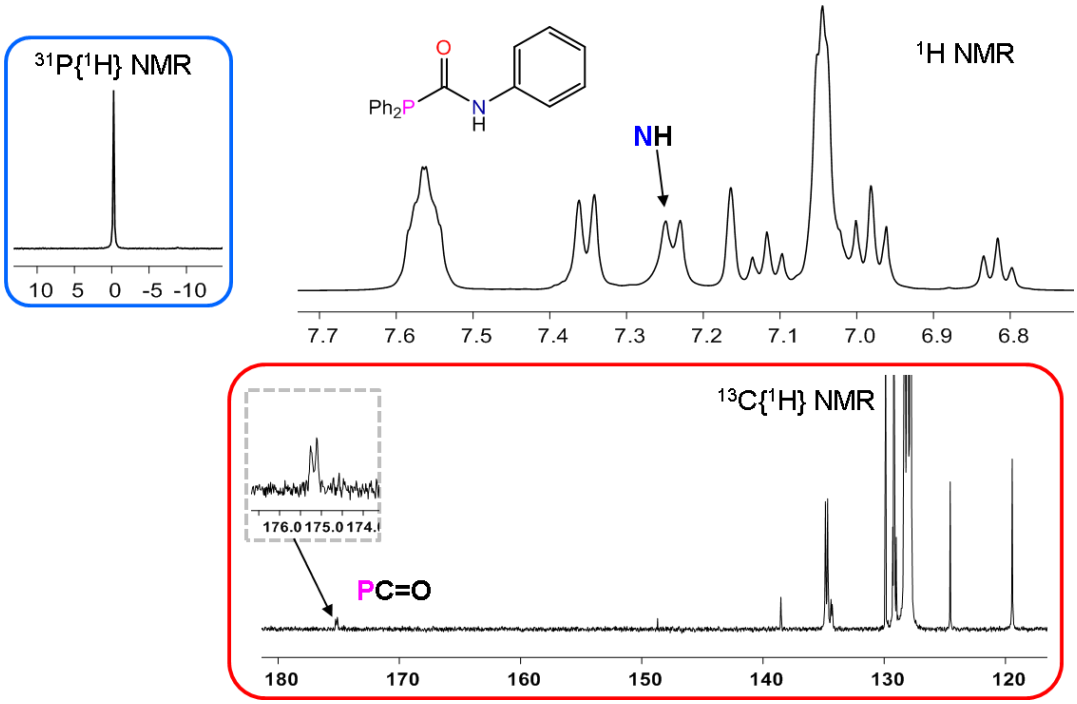

Figure S1. Selected region of the ^{1}H, $^{31}P\{^{1}H\}$ (framed in blue) and $^{13}C\{^{1}H\}$ (framed in red) NMR spectra complex of complex **3a** in C_6D_6. Spectroscopic data matched previous reported literature.[3]

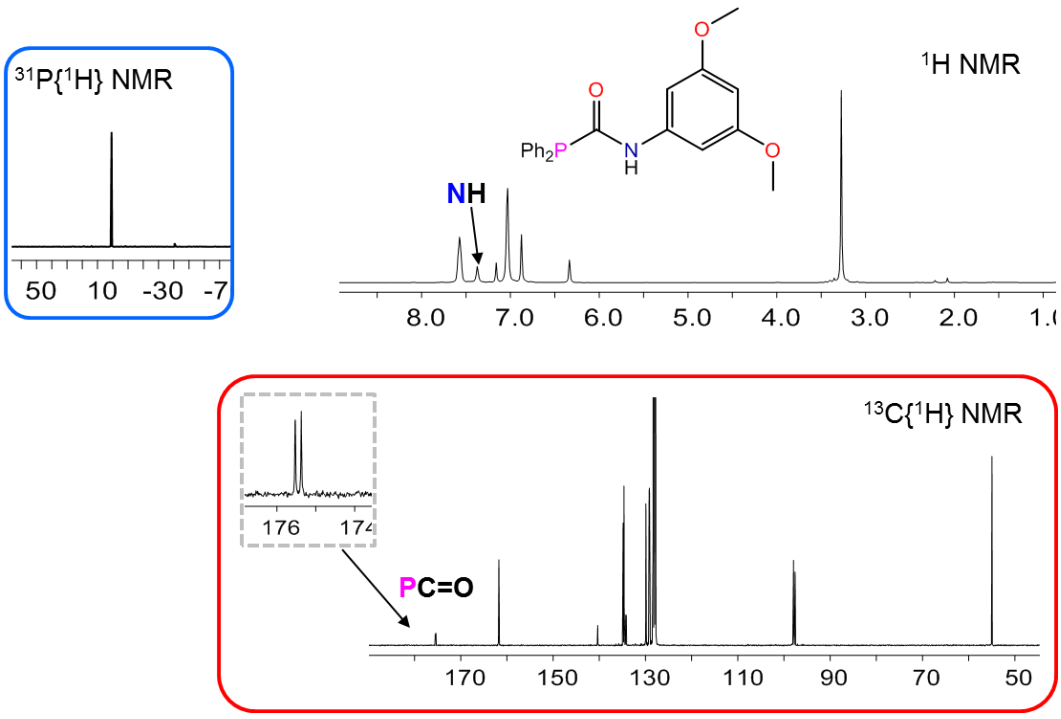

Figure S2. Selected region of the ^{1}H, $^{31}P\{^{1}H\}$ (framed in blue) and $^{13}C\{^{1}H\}$ (framed in red) NMR spectra complex of complex **3c** in C_6D_6.

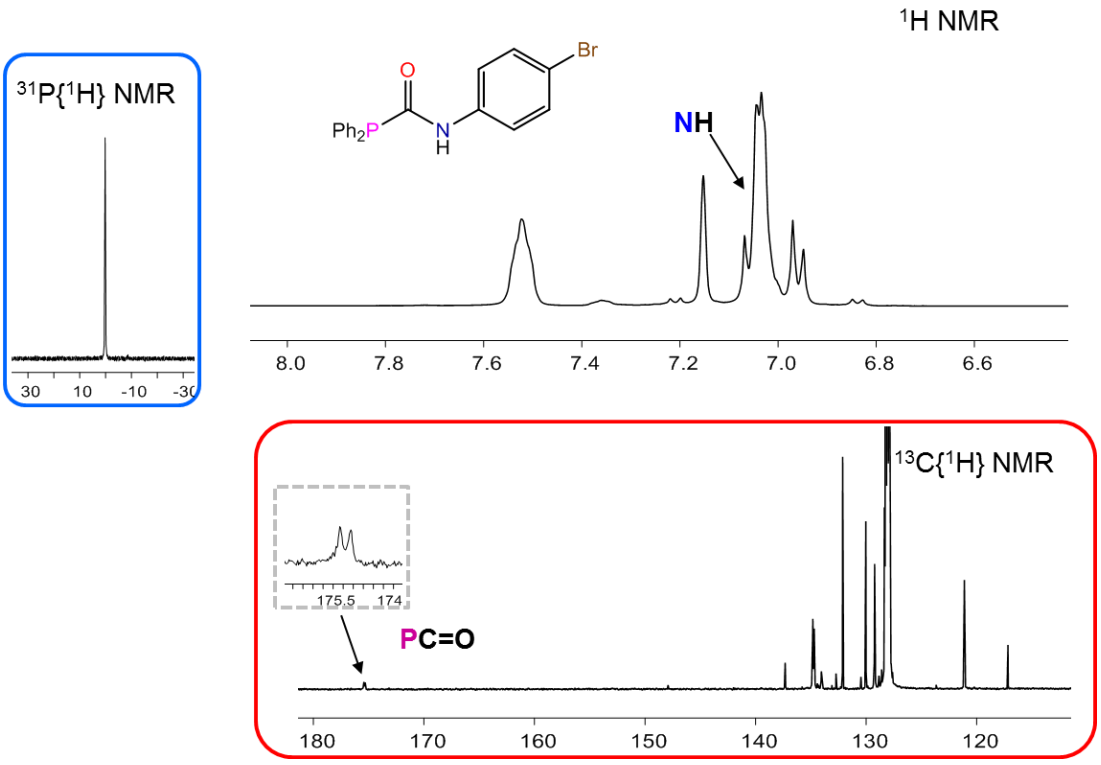

Figure S3. Selected region of the ^{1}H, $^{31}P\{^{1}H\}$ (framed in blue) and $^{13}C\{^{1}H\}$ (framed in red) complex of complex **3d** in C_6D_6. Spectroscopic data matched previous reported literature.[3]

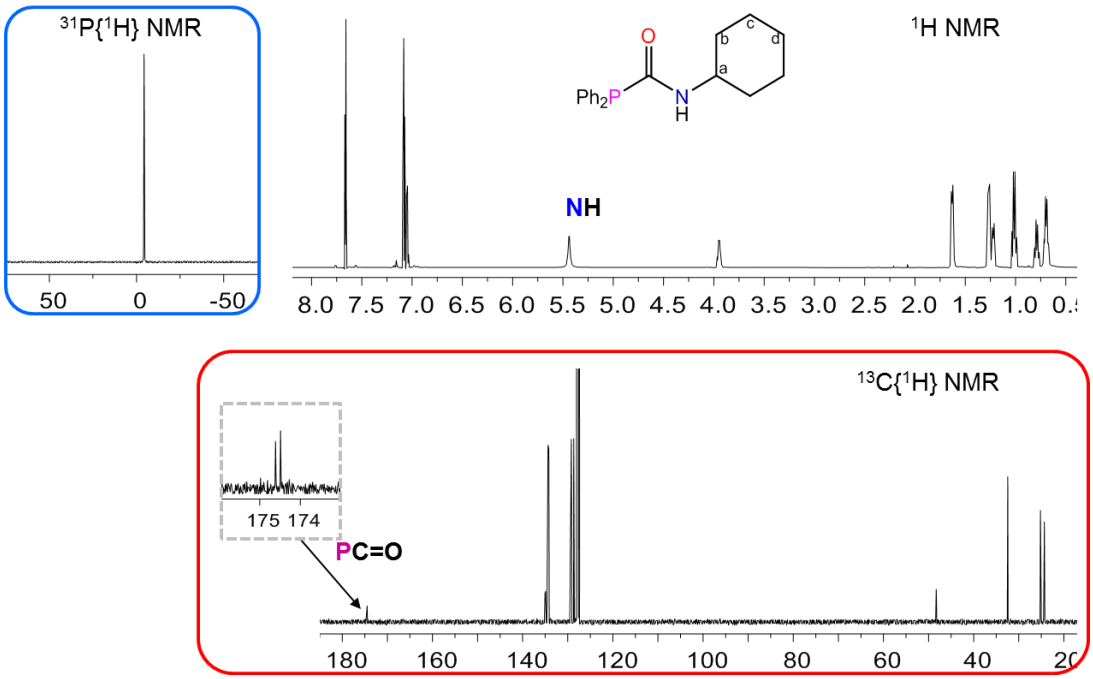

Figure S4. Selected region of the ^{1}H, $^{31}P\{^{1}H\}$ (framed in blue) and $^{13}C\{^{1}H\}$ (framed in red) NMR spectra complex of complex **3f** in C_6D_6. Spectroscopic data matched previous reported literature.[3]

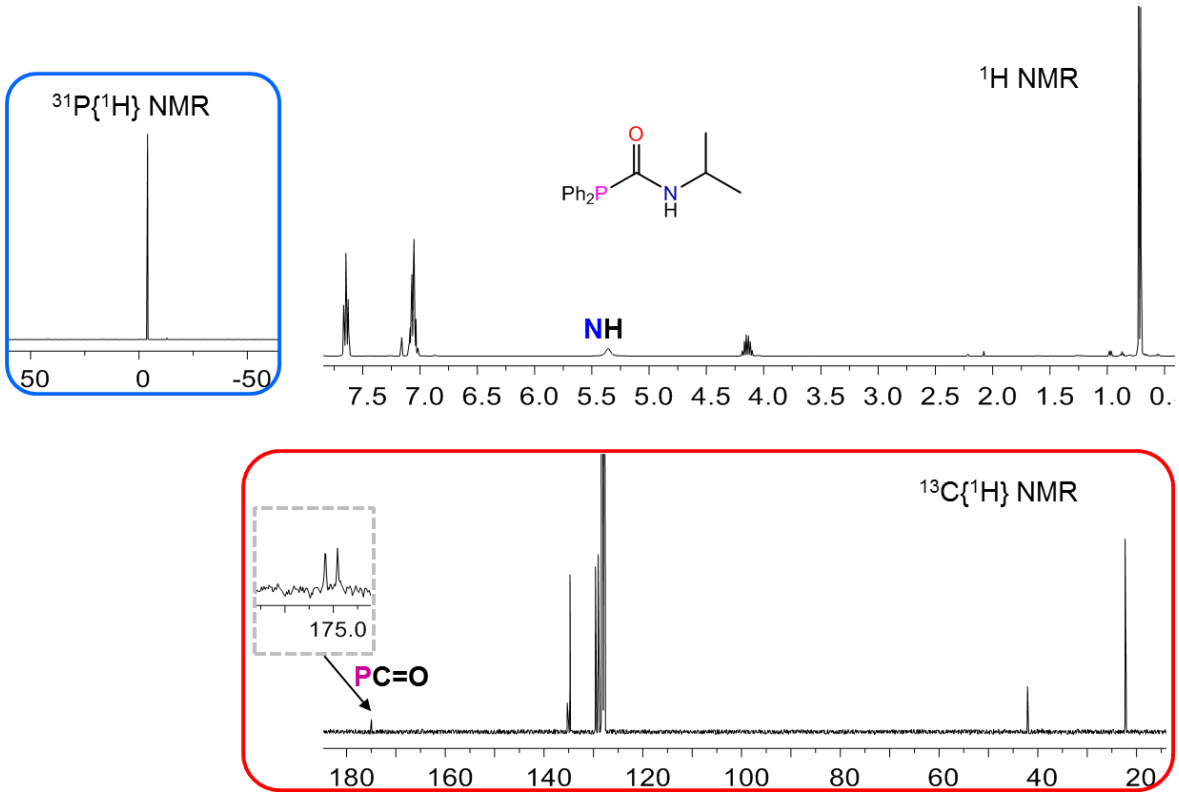

Figure S5. Selected region of the ^{1}H, $^{31}P\{^{1}H\}$ (framed in blue) and $^{13}C\{^{1}H\}$ (framed in red) NMR spectra complex of complex **3g** in C_6D_6.

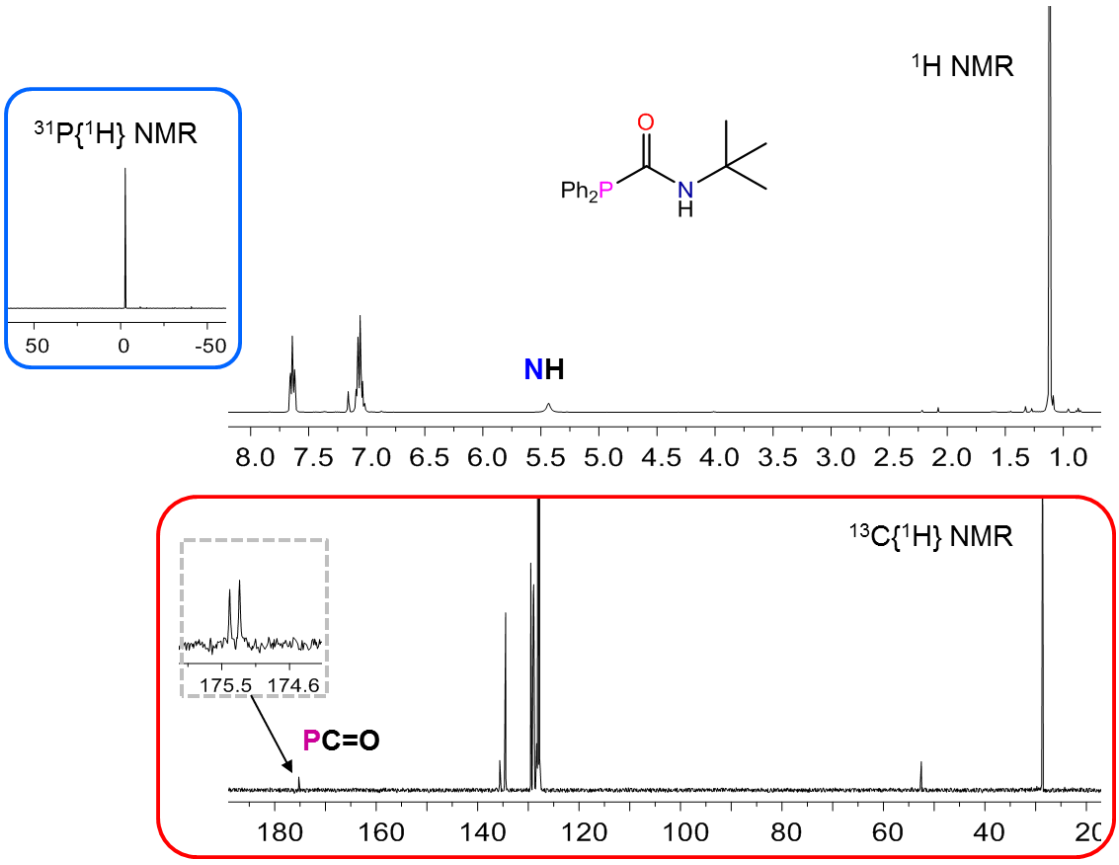

Figure S6. Selected region of the ^{1}H, $^{31}P\{^{1}H\}$ (framed in blue) and $^{13}C\{^{1}H\}$ (framed in red) NMR spectra complex of complex **3h** in C_6D_6.

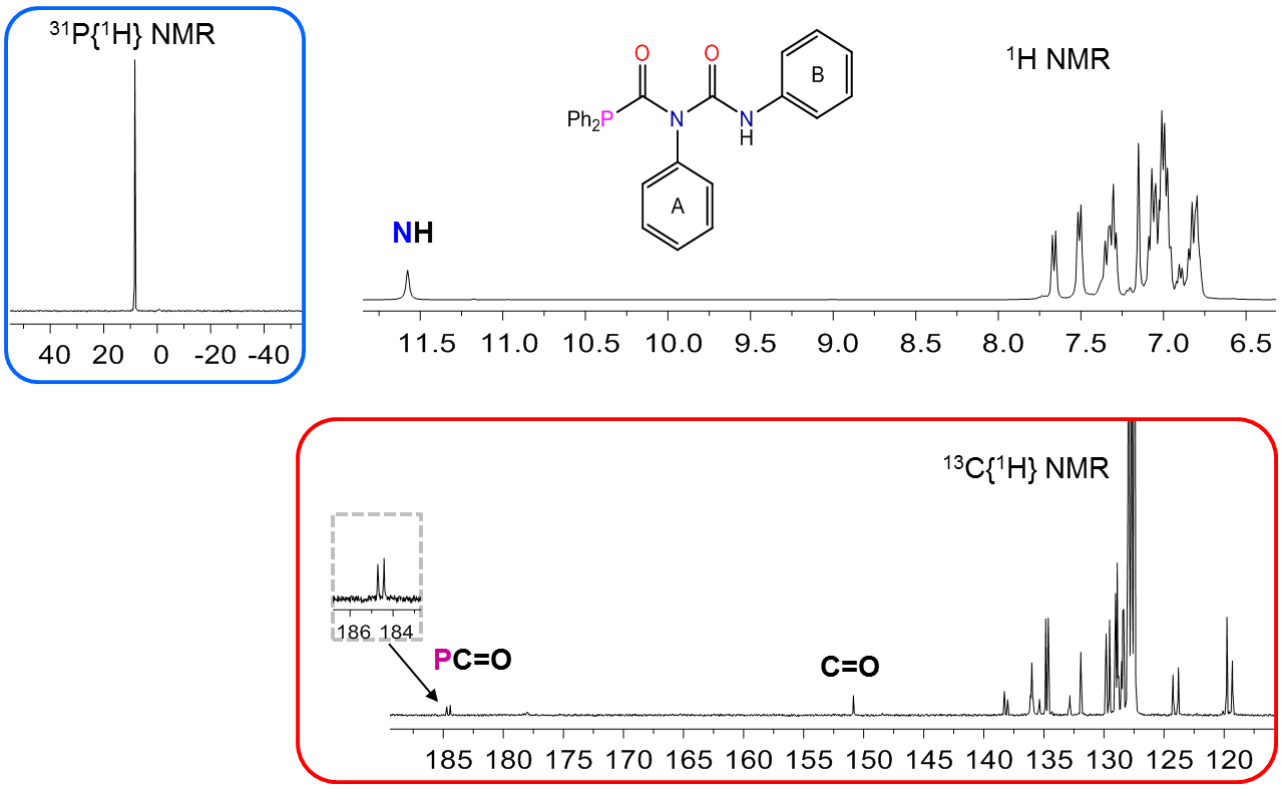

Figure S7. Selected region of the ^{1}H, $^{31}P\{^{1}H\}$ (framed in blue) and $^{13}C\{^{1}H\}$ (framed in red) NMR spectra complex of complex **4a** in C_6D_6.

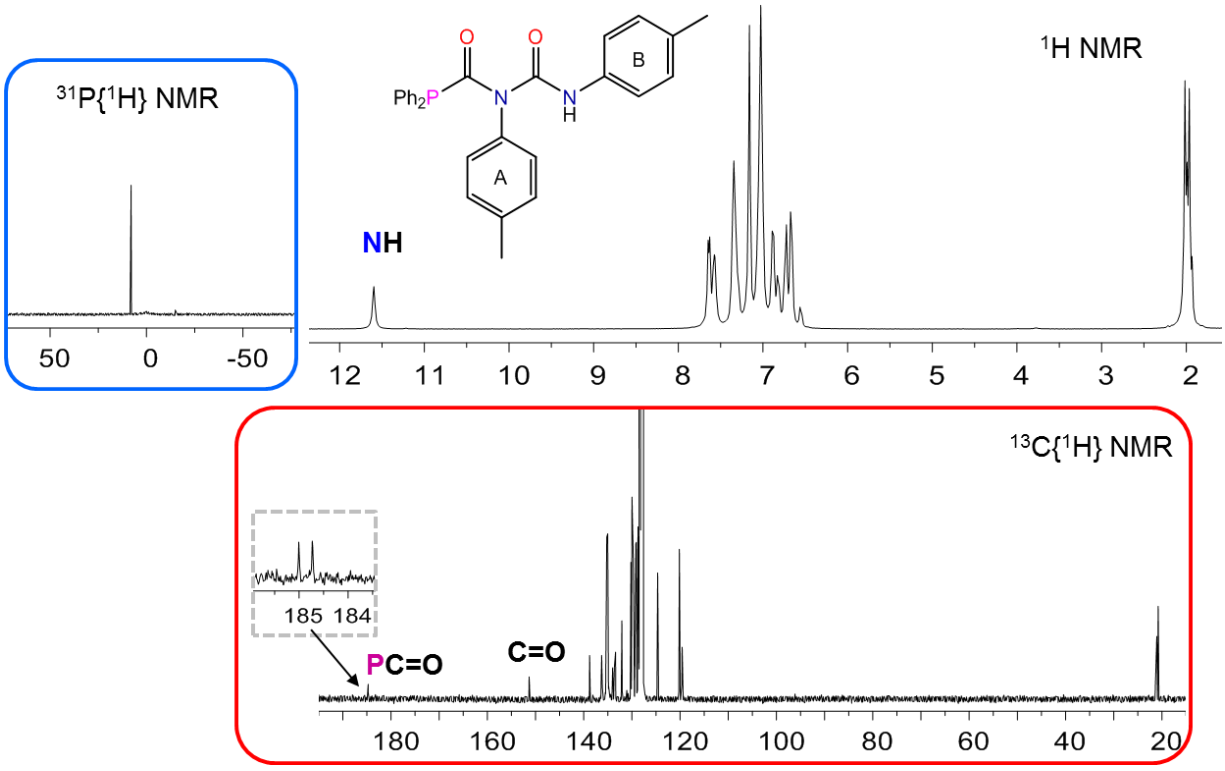

Figure S8. Selected region of the ^{1}H, $^{31}P\{^{1}H\}$ (framed in blue) and $^{13}C\{^{1}H\}$ (framed in red) NMR spectra complex of complex **4b** in C_6D_6.

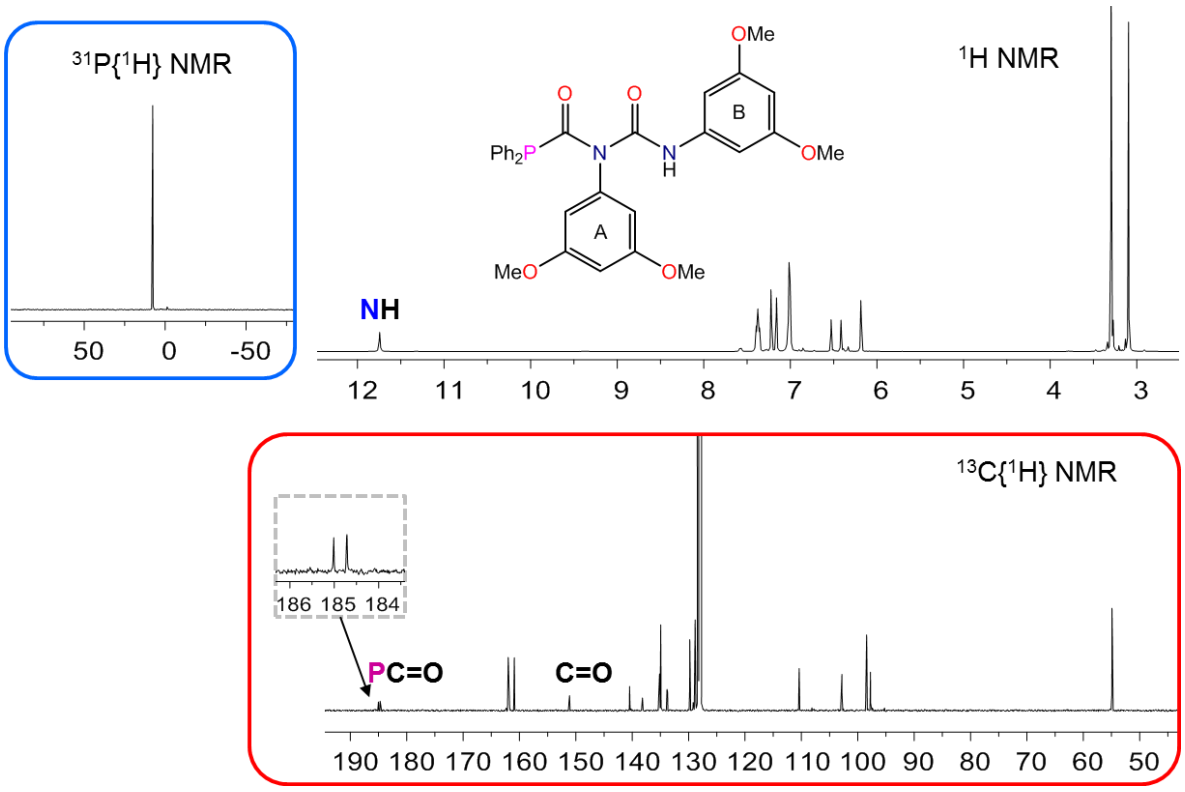

Figure S9. Selected region of the ^{1}H, $^{31}P\{^{1}H\}$ (framed in blue) and$^{13}C\{^{1}H\}$ (framed in red) NMR spectra complex of complex **4c** in C_6D_6.

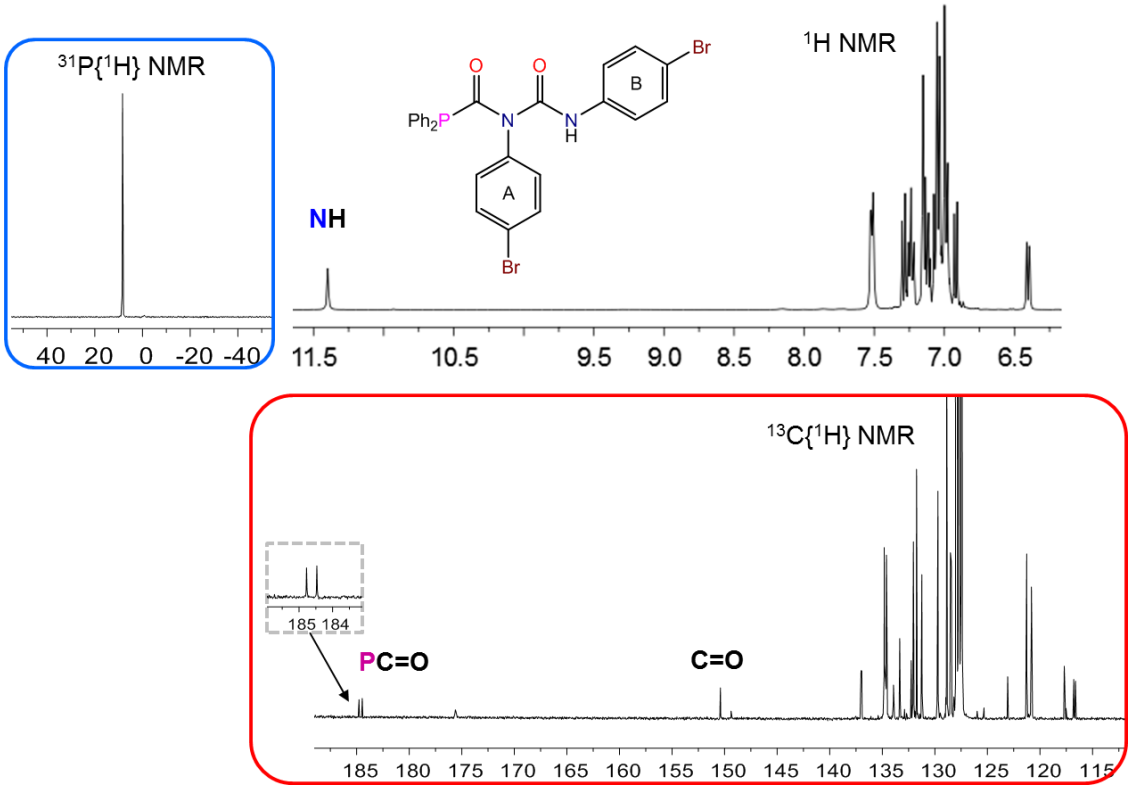

Figure S10. Selected region of the ^{1}H, $^{31}P\{^{1}H\}$ (framed in blue) and $^{13}C\{^{1}H\}$ (framed in red) NMR spectra complex of complex **4d** in C_6D_6.

NMR Reaction Monitoring

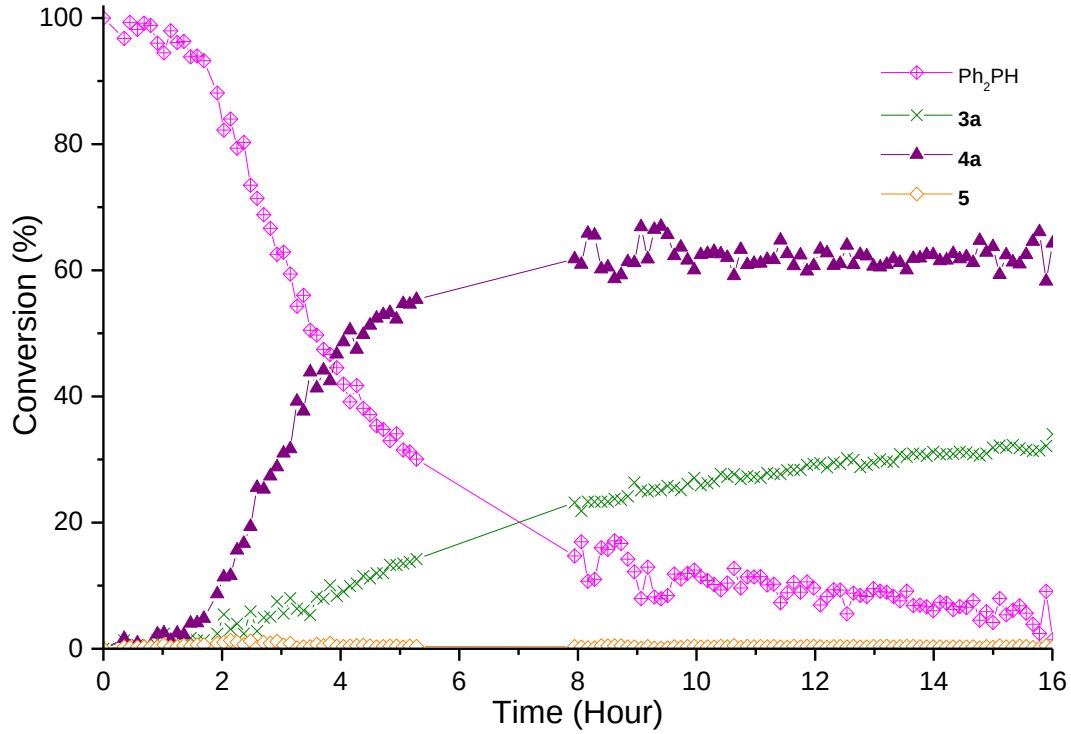

Figure S11. Conversion (%) *vs.* time (hour) for the hydrophosphination of PhNCO with 5 mol% cat. of **1** in C_6D_6 at 25 °C.

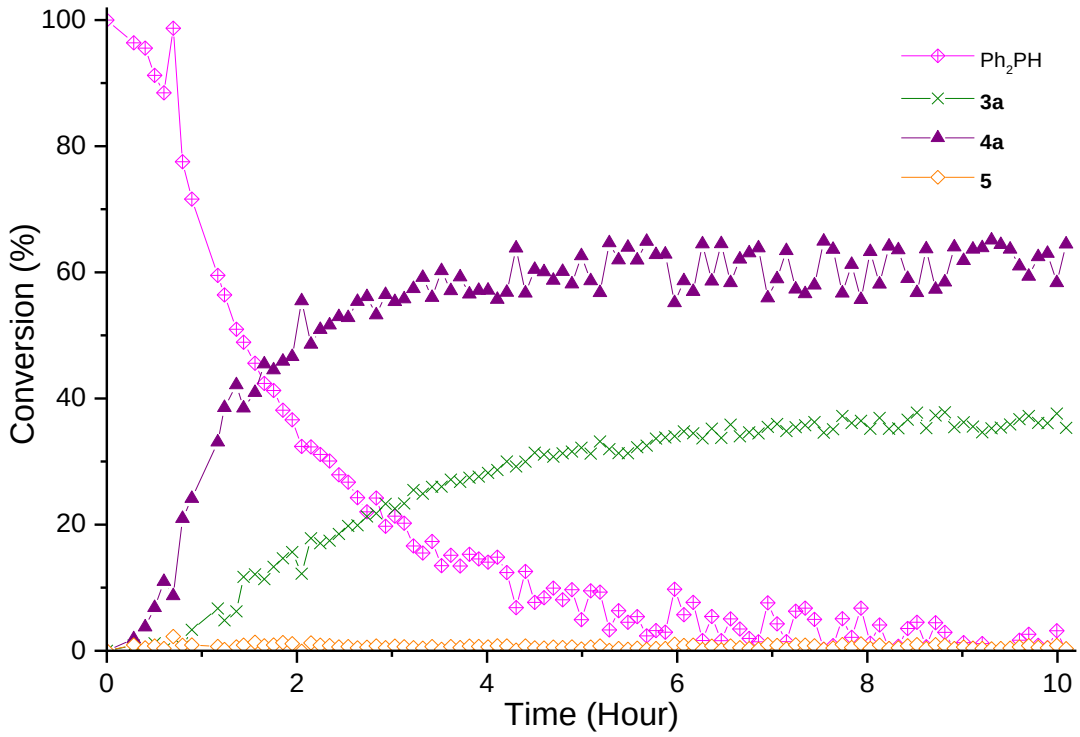

Figure S12. Conversion (%) *vs.* time (hour) for the hydrophosphination of PhNCO with 5 mol% cat. of **2** in C_6D_6 at 25 °C.

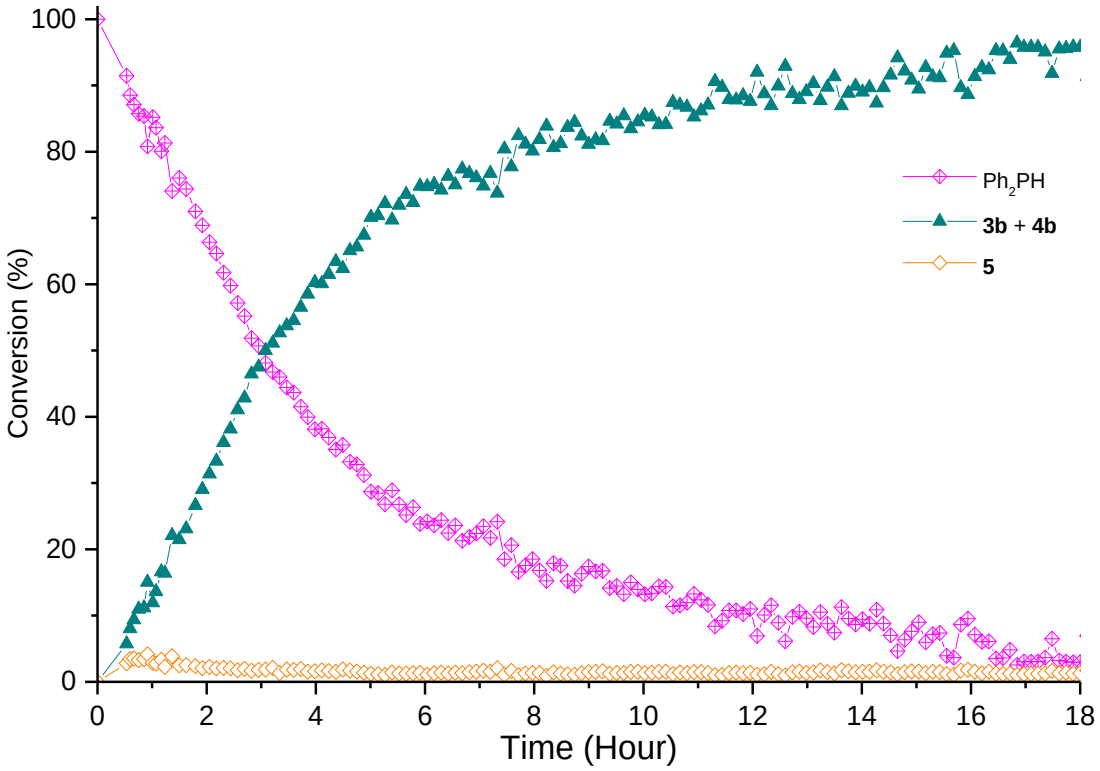

Figure S13. Conversion (%) *vs.* time (hour) for the hydrophosphination of ^{p}TolNCO with 5 mol% cat. of **1** in C_6D_6 at 25 °C. Peaks for **3** and **4** overlapped in the $^{31}P\{^{1}H\}$ NMR spectra.

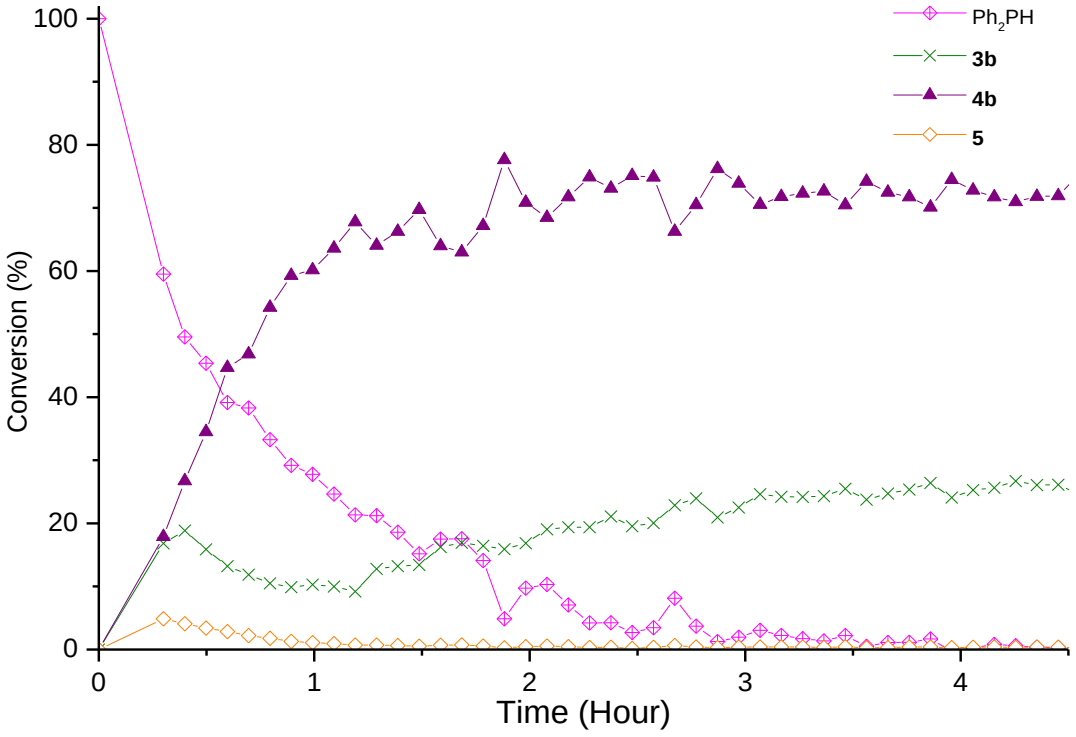

Figure S14. Conversion (%) *vs.* time (hour) for the hydrophosphination of ^{p}TolNCO with 5 mol% cat. of **2** in C_6D_6 at 25 °C.

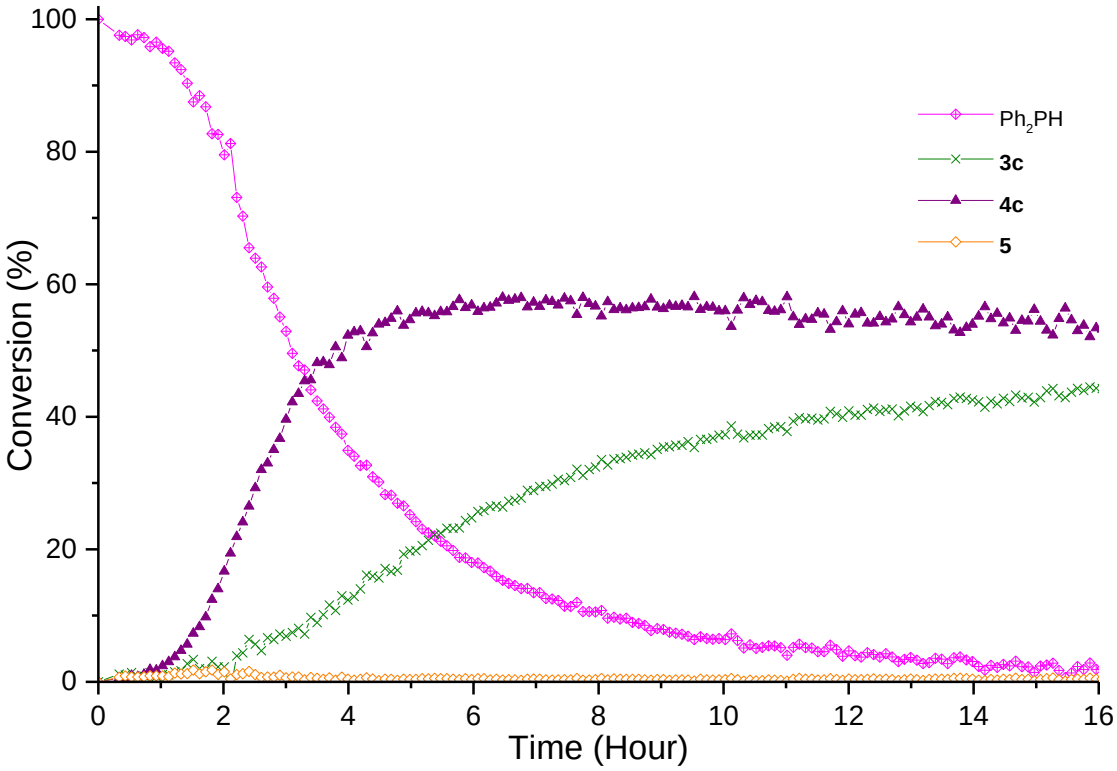

Figure S15. Conversion (%) *vs.* time (hour) for the hydrophosphination of 3,5-$(OMe)_2C_6H_3NCO$ with 5 mol% cat. of **1** in C_6D_6 at 25 °C.

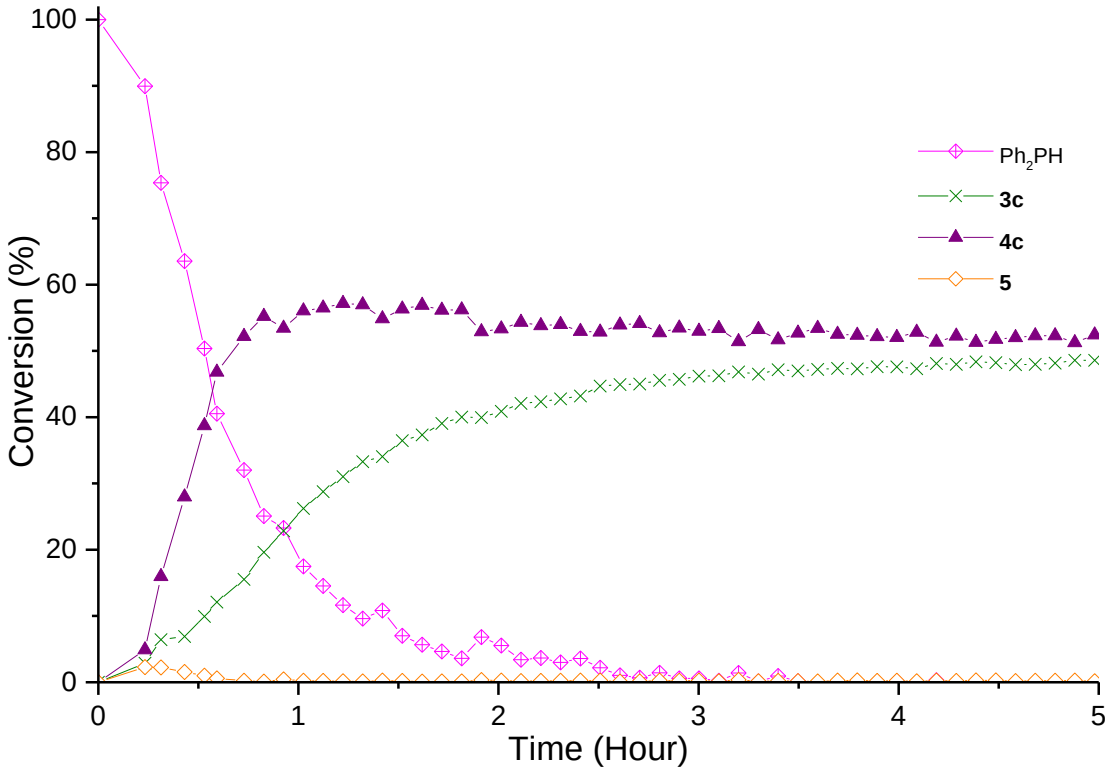

Figure S16. Conversion (%) *vs.* time (hour) for the hydrophosphination of 3,5-$(OMe)_2C_6H_3NCO$ with 5 mol% cat. of **2** in C_6D_6 at 25 °C.

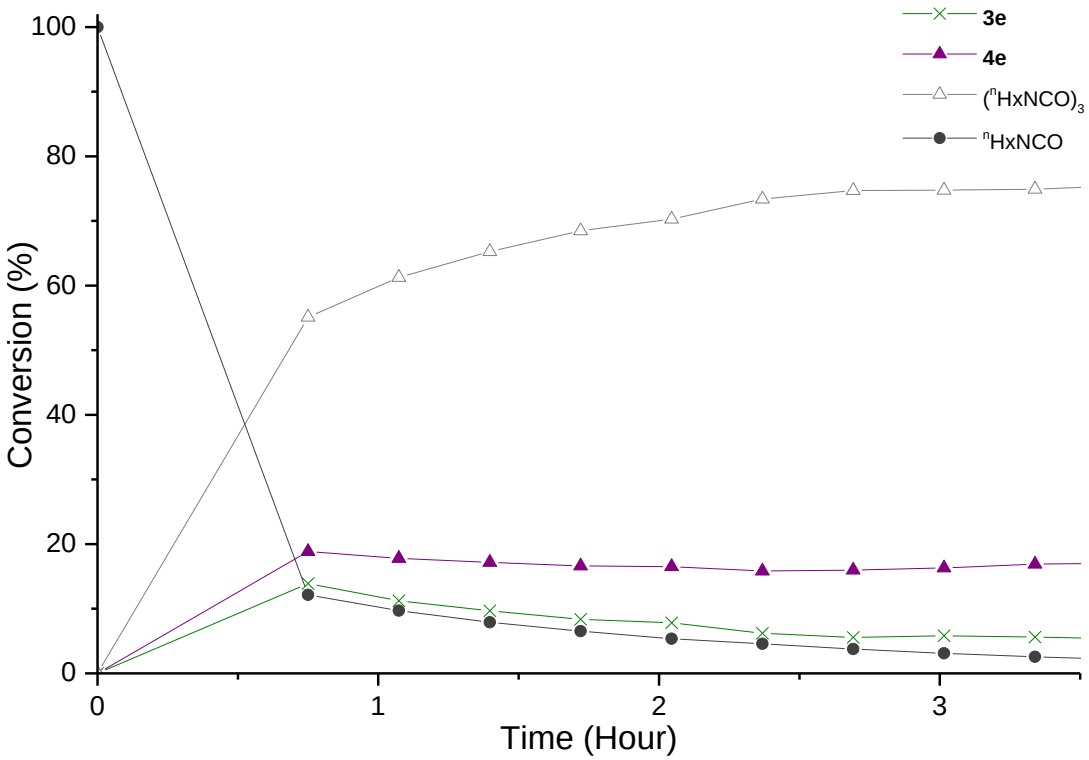

Figure S17. Conversion (%) *vs.* time (hour) for the hydrophosphination of ^{n}HxNCO with 5 mol% cat. of **1** in C_6D_6 at 25 °C. Reaction followed by ^{1}H NMR.

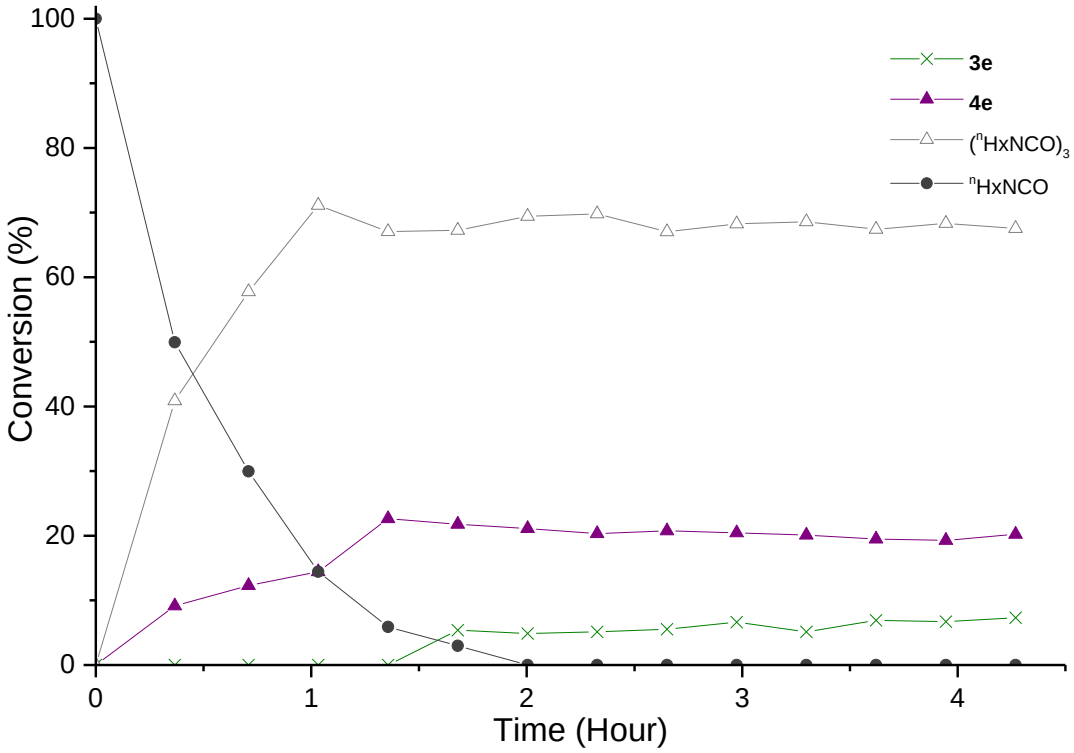

Figure S18. Conversion (%) *vs.* time (hour) for the hydrophosphination of ^{n}HxNCO with 5 mol% cat. of **2** in C_6D_6 at 25 °C. Reaction followed by ^{1}H NMR.

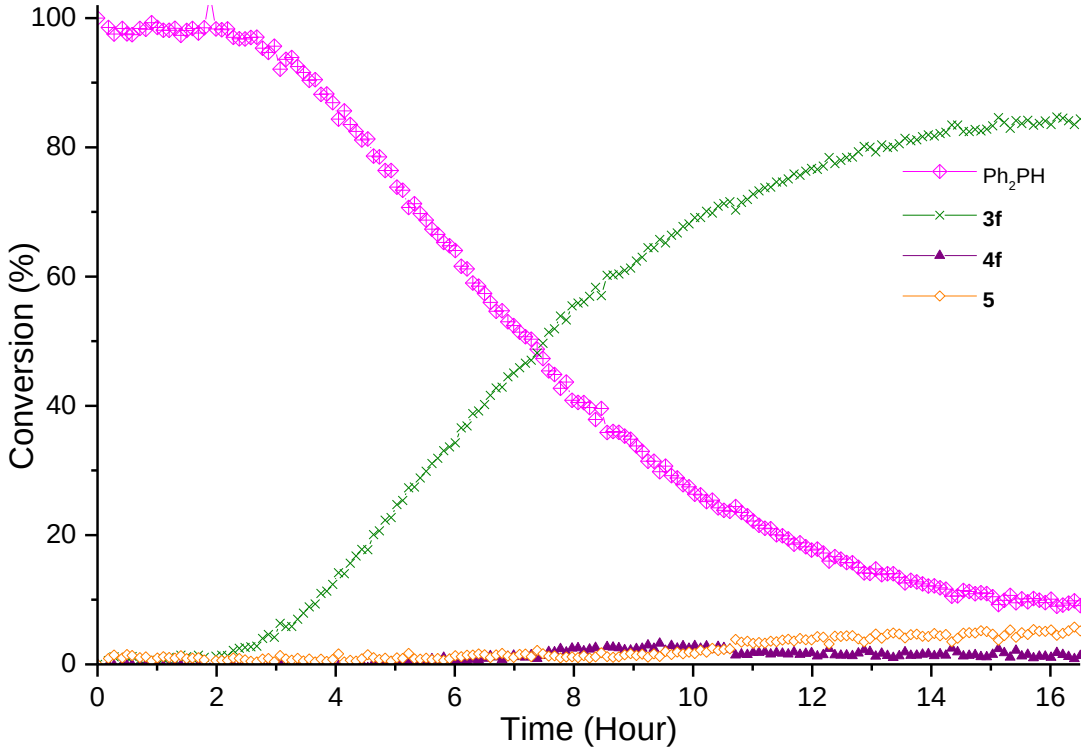

Figure S19. Conversion (%) *vs.* time (hour) for the hydrophosphination of CyNCO with 5 mol% cat. of **1** in C_6D_6 at 25 °C.

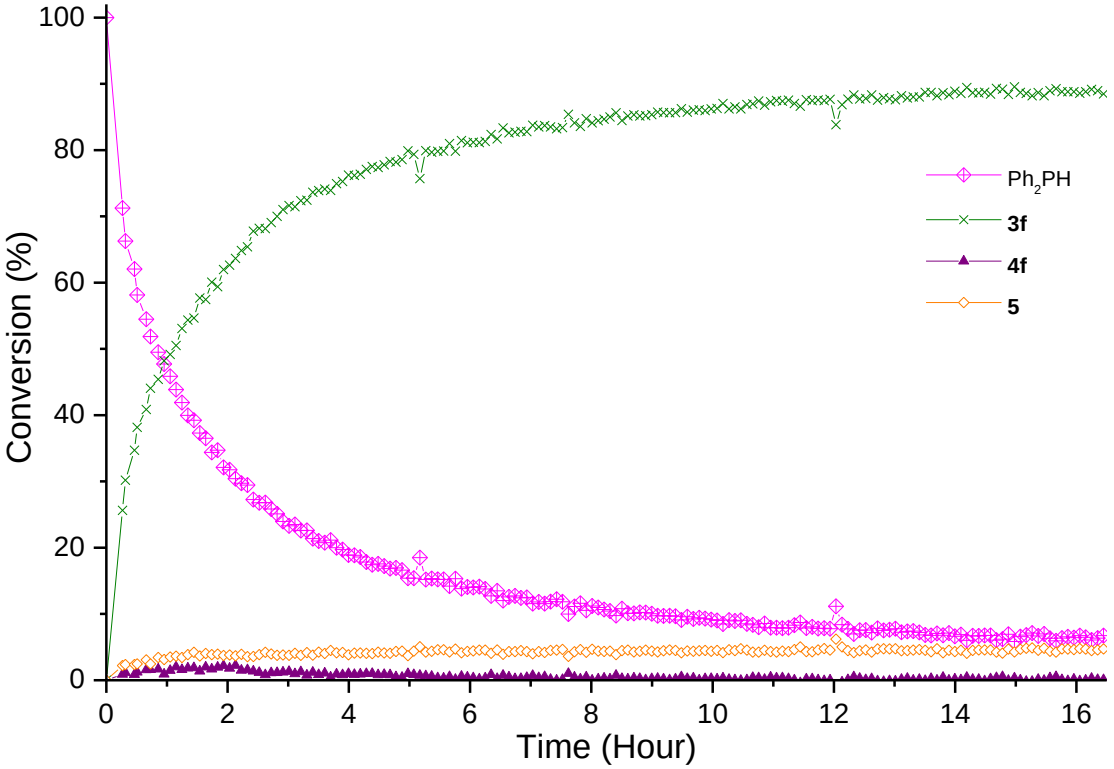

Figure S20. Conversion (%) *vs.* time (hour) for the hydrophosphination of CyNCO with 5 mol% cat. of **2** in C_6D_6 at 25 °C.

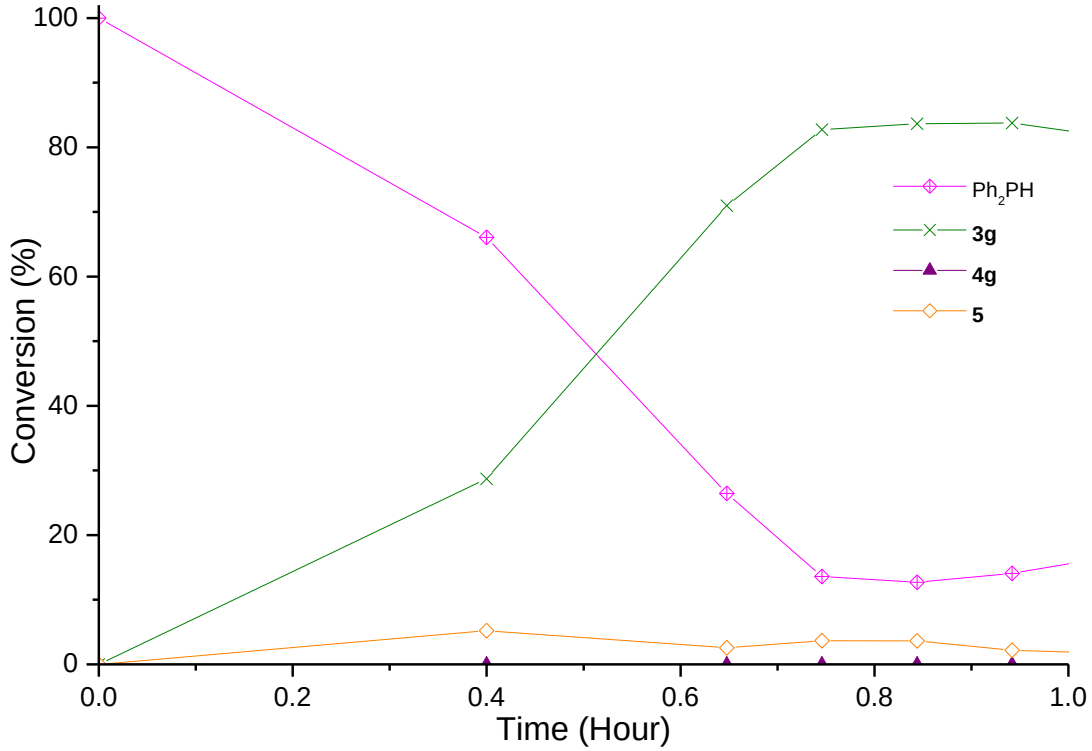

Figure S21. Conversion (%) *vs.* time (hour) for the hydrophosphination of ^{i}PrNCO with 5 mol% cat. of **1** in C_6D_6 at 60 °C.

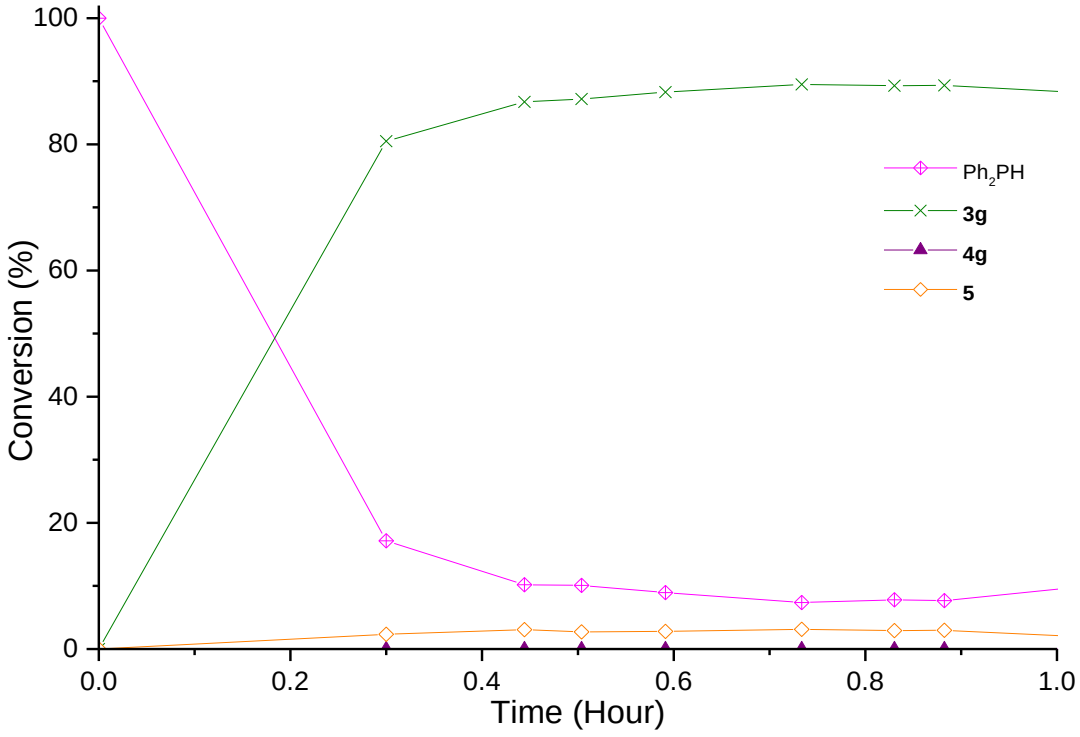

Figure S22. Conversion (%) *vs.* time (hour) for the hydrophosphination of ^{i}PrNCO with 5 mol% cat. of **2** in C_6D_6 at 60 °C.

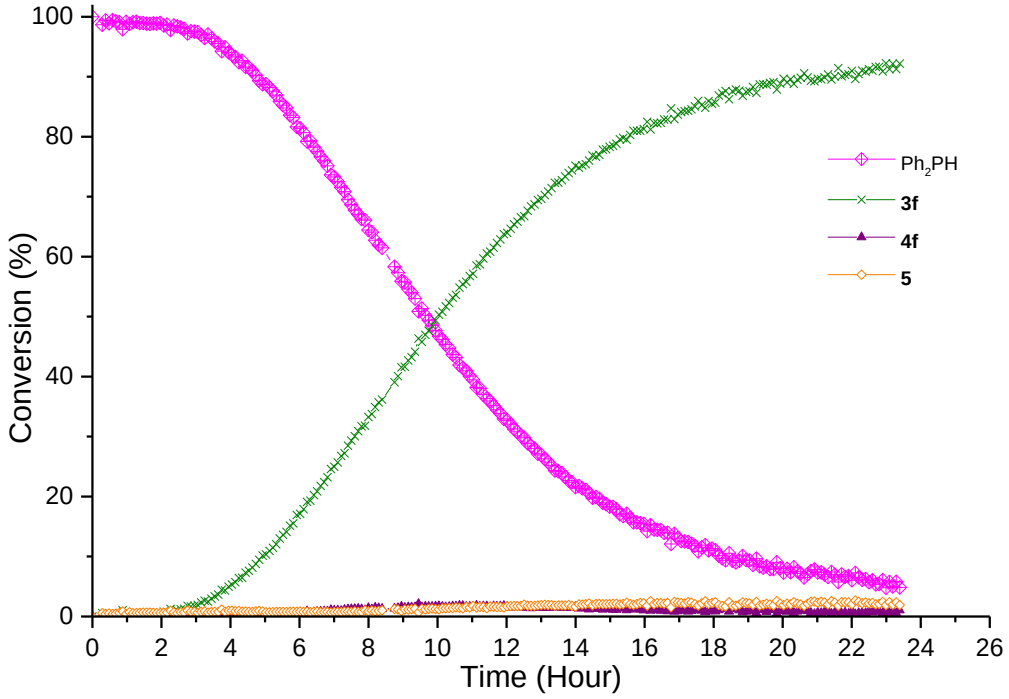

Figure S23. Conversion (%) *vs.* time (hour) for the hydrophosphination of CyNCO with 5 mol% cat. of **1** in C_6D_6 at 25 °C with a drop of mercury.

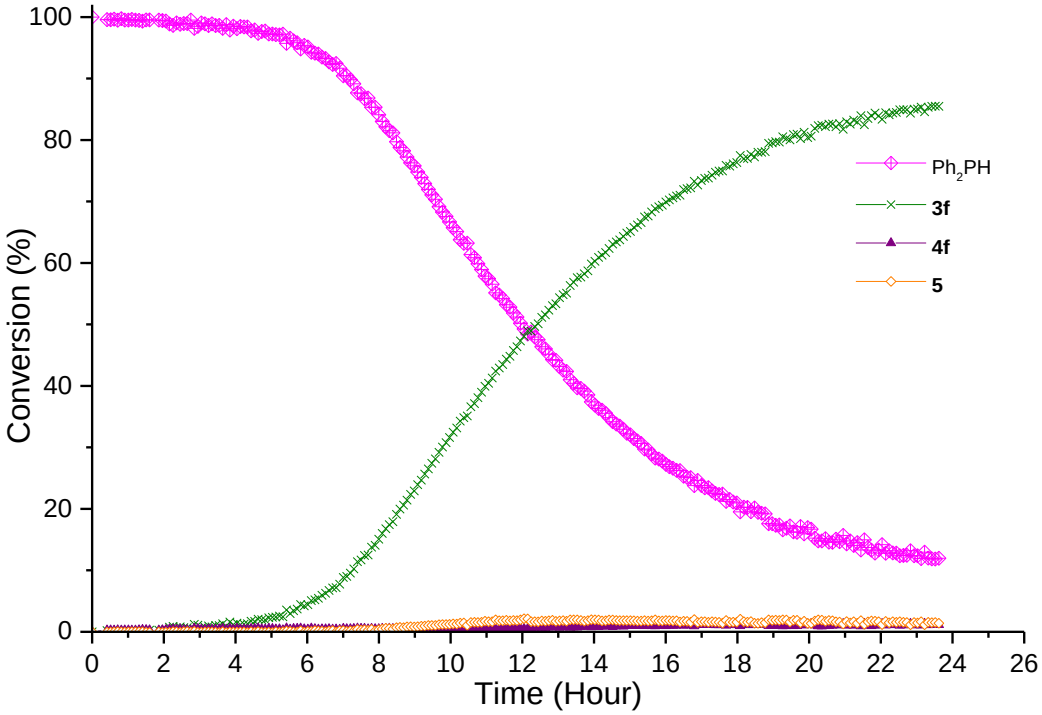

Figure S24. Conversion (%) *vs.* time (hour) for the hydrophosphination of CyNCO with 5 mol% cat. of **1** in C_6D_6 at 25 °C with CS_2.

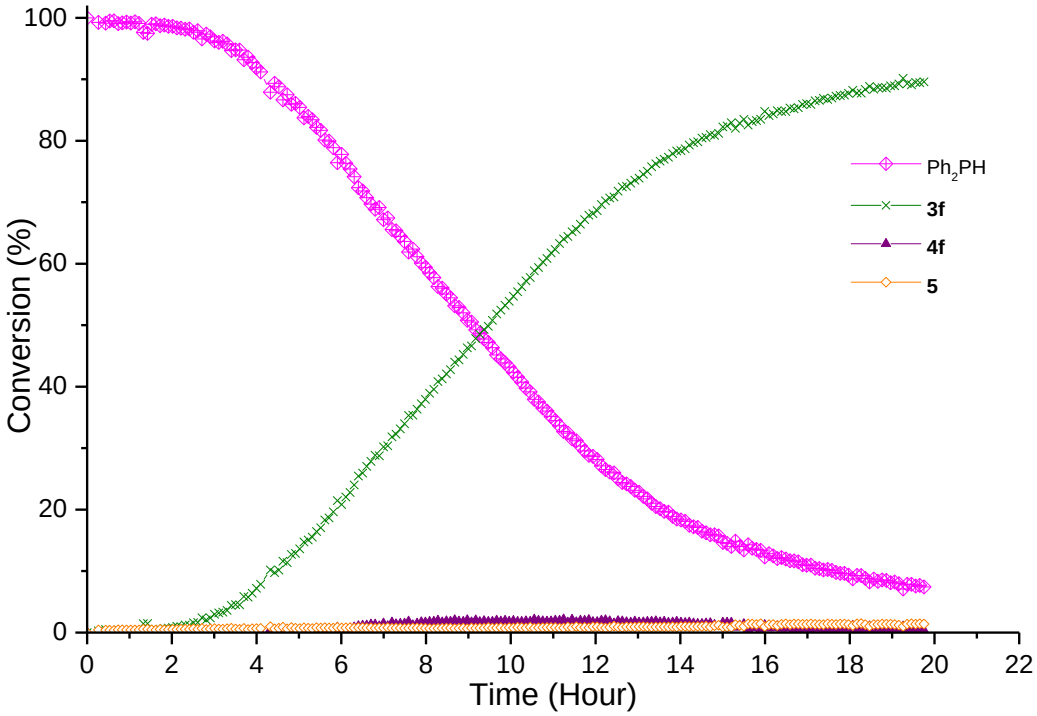

Figure S25. Conversion (%) *vs.* time (hour) for the hydrophosphination of CyNCO with 5 mol% cat. of **1** in C_6D_6 at 25 °C with an excess of cumene.

X-ray Structure Analyses

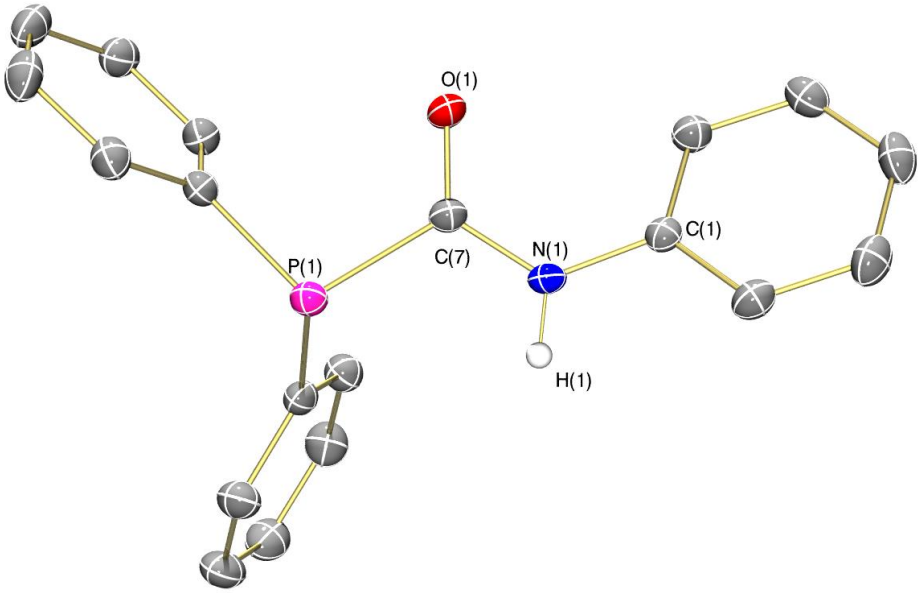

Figure S26. Molecular structure of **3a** with anisotropic displacement parameters set at 50% probability. Hydrogen atoms [with the exception of H(1)] have been omitted for clarity.

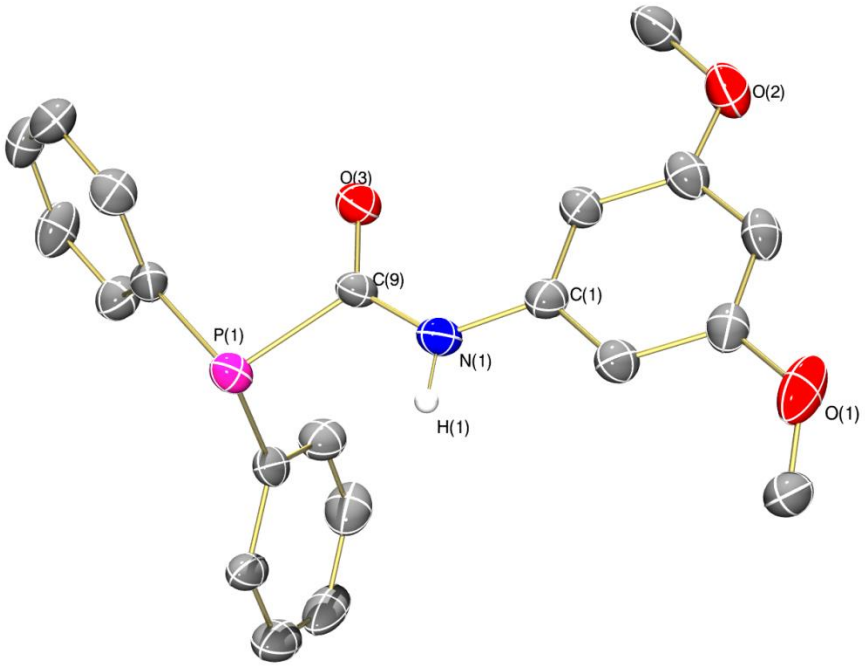

Figure S27. Molecular structure of **3c** with anisotropic displacement parameters set at 50% probability. Hydrogen atoms [with the exception of H(1)] and minor disorder components of the molecule have been omitted for clarity.

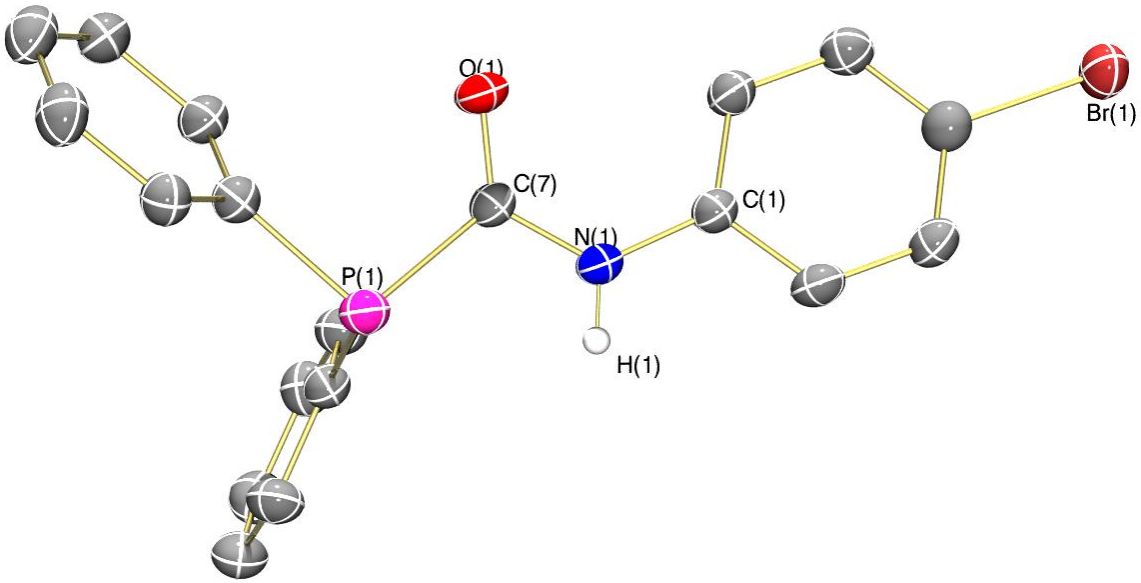

Figure S28. Molecular structure of **3d** with anisotropic displacement parameters set at 50% probability. Hydrogen atoms [with the exception of H(1)] and minor disorder components of the molecule have been omitted for clarity

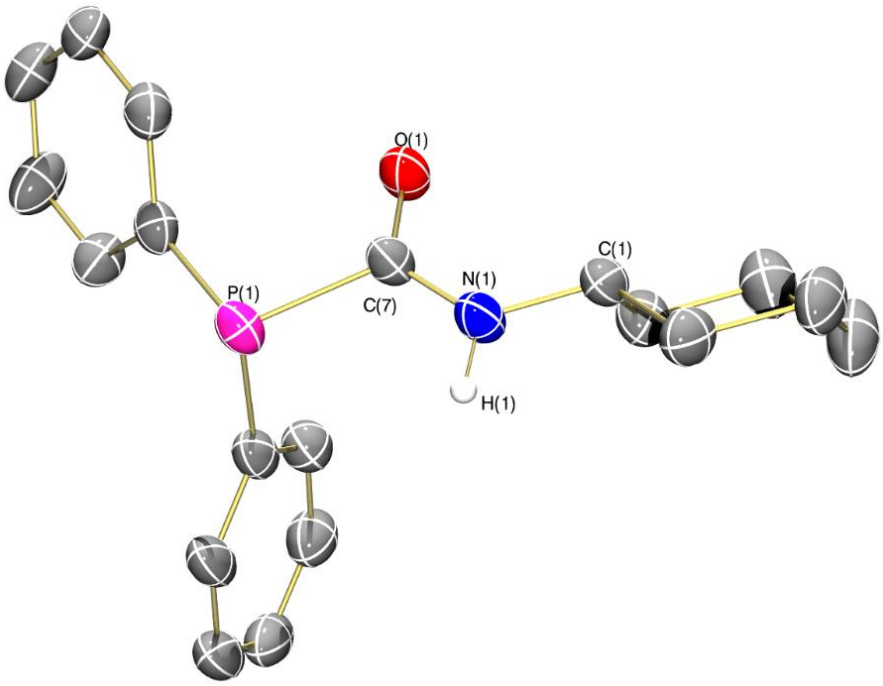

Figure S29. Molecular structure of **3f** anisotropic displacement parameters set at 50% probability. Hydrogen atoms [with the exception of H(1)] have been omitted for clarity.

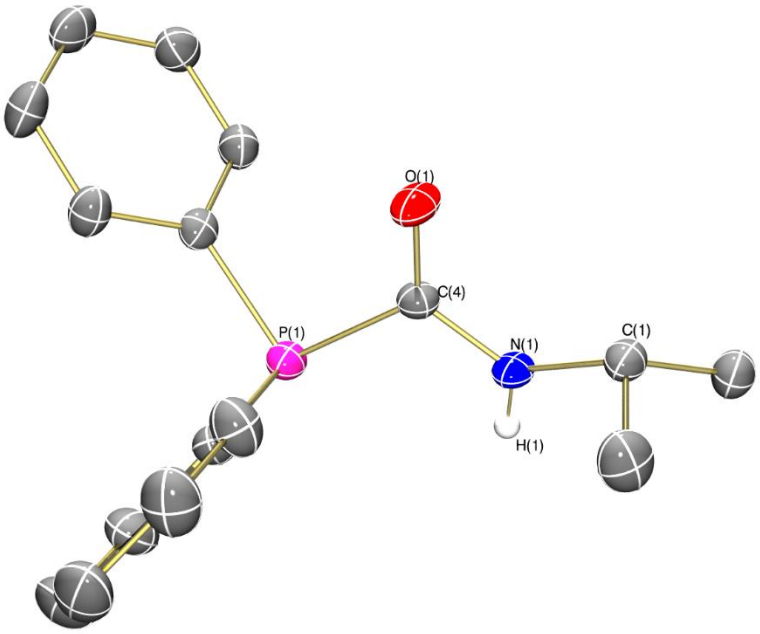

Figure S30. Molecular structure of **3g** with anisotropic displacement parameters set at 50% probability. Hydrogen atoms [with the exception of H(1)] have been omitted for clarity.

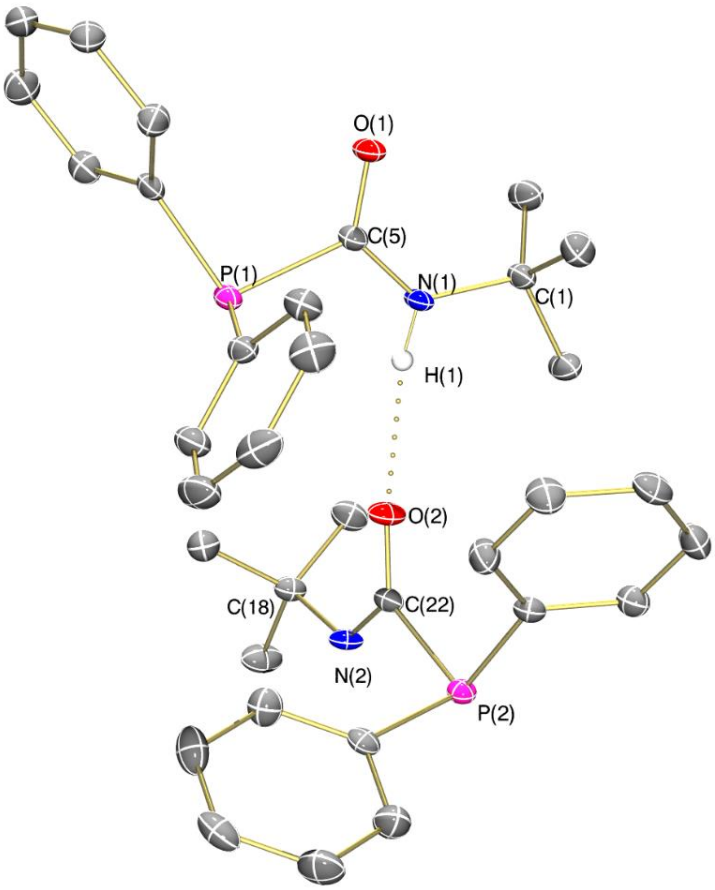

Figure S31. Molecular structure of **3h** anisotropic displacement parameters set at 50% probability. Hydrogen atoms [with the exception of H(1)] have been omitted for clarity.

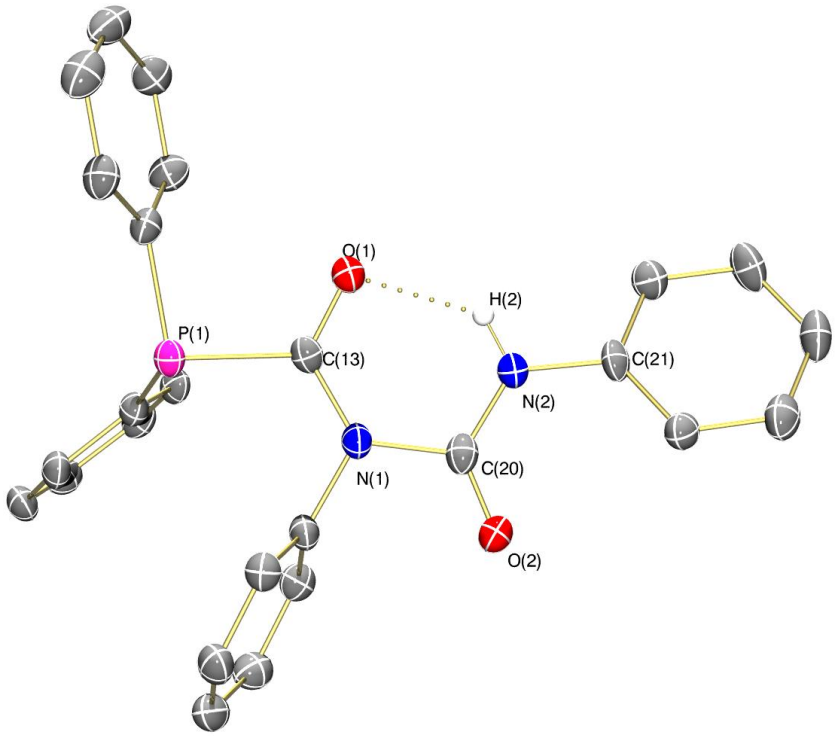

Figure S32. Molecular structure of **4a** with anisotropic displacement parameters set at 50% probability. Hydrogen atoms [with the exception of H(2)] have been omitted for clarity.

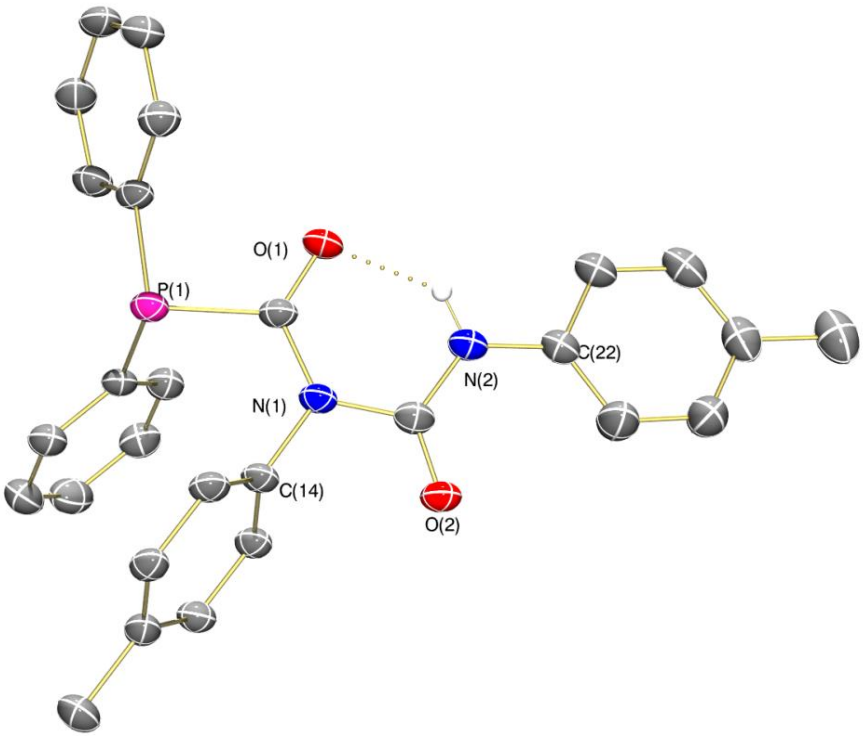

Figure S33. Molecular structure of **4b** with anisotropic displacement parameters set at 50% probability. Hydrogen atoms [with the exception of H(2)] have been omitted for clarity.

Crystallographic Methods

Under a flow of nitrogen, crystals suitable for analysis by X-ray diffraction were quickly removed from the crystallisation vessel and covered in YR-1800 perfluoropolyether oil. Crystals were mounted on a MiTeGen MicroMount™ and cooled rapidly in a cold stream of nitrogen using an Oxford Cryostreams open flow cryostat.[4] Single crystal X-ray diffraction data were collected on Rikagu Oxford Diffraction SuperNova diffractometer (mirror-monochromated Cu-Kα radiation source; λ = 1.54184 Å; ω scans), equipped with either an Atlas, AtlasS2 or TitanS2 detector. Cell parameters were refined from the observed positions of all strong reflections in each data set and absorption corrections were applied using a Gaussian numerical method with beam profile correction (CrysAlisPro).[5] The structures were solved either by direct or iterative methods and all non-hydrogen atoms refined by full-matrix least-squares on all unique F^2 values with anisotropic displacement parameters. Hydrogen atoms were refined with constrained geometries and riding thermal parameters with the exception of amide hydrogen atoms whose positions were refined freely. Programs used include CrysAlisPro[5] (control of Supernova, data integration and absorption correction), SHELXL[6] (structure refinement), SHELXS[7] (structure solution), SHELXT[8] (structure solution), OLEX2[9] (molecular graphics). Structure **3d** was a 2-component twin. The orientations of the two twin components were determined in CryAlisPro,[5] and integrated to provide a single component HKL file which was used for the initial solution, and a multi-component HKL file which was used for the final refinement of the structure. CIF files were checked using checkCIF.[10] CCDC-1529760-1529767 contain the supplementary data for **3a**,**c**,**d**,**f**-**h** and **4a**,**b**. These data can be obtained free of charge from The Cambridge Crystallographic Data Centre *via* www.ccdc.cam.ac.uk/data_request/cif.

Crystal data for $PPh_2C(=O)NH(Ph)$ (3a)

$C_{19}H_{16}NOP$ (M =305.30 g/mol): orthorhombic, space group *Pbca* (no. 61), a = 10.3671(4), b = 9.7004(3), c = 30.7223(11) Å, V = 3089.59(18) Å^3, Z = 8, T = 120(2) K, μ(Cu-$K\alpha$) = 1.573 mm^{-1}, D_{calc} = 1.313 g/cm^3, 7371 reflections measured (10.294° ≤ 2Θ ≤ 148.912°), 3060 unique (R_{int} = 0.0244, R_{sigma} = 0.0281) which were used in all calculations. The final R_1 was 0.0348 ($I > 2\sigma(I)$) and wR_2 was 0.0916 (all data).

Crystal data for $PPh_2C(=O)NH(3,5\text{-}(OMe)_2C_6H_3)$ (3c)

$C_{21}H_{20}NO_3P$ (M = 365.35 g/mol): orthorhombic, space group *Iba*2 (no. 45), a = 37.803(3), b = 10.3736(7), c = 9.4895(7) Å, V = 3721.3(5) Å^3, Z = 8, T = 120(2) K, μ(Cu-$K\alpha$) = 1.476 mm^{-1}, D_{calc} = 1.304 g/cm^3, 4993 reflections measured (8.84° ≤ 2Θ ≤ 149.442°), 2553 unique (R_{int} = 0.0440, R_{sigma} = 0.0483) which were used in all calculations. The final R_1 was 0.0661 (I > 2σ(I)) and wR_2 was 0.1754 (all data).

Crystal data for $PPh_2C(=O)NH(4\text{-}BrC_6H_4)$ (3d)

$C_{19}H_{15}NOPBr$ (M = 384.20 g/mol): monoclinic, space group $P2_1/c$ (no. 14), a = 16.4956(7), b = 10.3340(5), c = 9.7346(4) Å, β = 94.043(4)°, V = 1655.28(13) Å^3, Z = 4, T = 120(2) K, μ(Cu-$K\alpha$) = 4.319 mm^{-1}, D_{calc} = 1.542 g/cm^3, 6619 reflections measured (10.108° ≤ 2Θ ≤ 148.846°), 6619 unique (R_{sigma} = 0.0260) which were used in all calculations. The final R_1 was 0.0729 (I > 2σ(I)) and wR_2 was 0.208 (all data).

Crystal data for $PPh_2C(=O)NH(Cy)$ (3f)

$C_{19}H_{22}NOP$ (M = 311.34 g/mol): orthorhombic, space group *Iba*2 (no. 45), a = 34.1888(3), b = 10.64763(8), c = 9.49011(9) Å, V = 3454.68(5) Å^3, Z = 8, T = 120(2) K, μ(Cu-$K\alpha$) = 1.408 mm^{-1}, D_{calc} = 1.197 g/cm^3, 37101 reflections measured (8.698° ≤ 2Θ ≤ 147.574°), 3273 unique (R_{int} = 0.0426, R_{sigma} = 0.0151) which were used in all calculations. The final R_1 was 0.0360 (I > 2σ(I)) and wR_2 was 0.0949 (all data).

Crystal data for $PPh_2C(=O)NH(^i Pr)$ (3g)

$C_{16}H_{18}NOP$ (M = 271.28 g/mol): orthorhombic, space group *Pbca* (no. 61), a = 11.1668(2), b = 9.5381(2), c = 28.3885(5) Å, V = 3023.67(10) Å^3, Z = 8, T = 120(2) K, μ(Cu-$K\alpha$) = 1.536 mm^{-1}, D_{calc} = 1.192 g/cm^3, 15166 reflections measured (10.078° ≤ 2Θ ≤ 147.404°), 3017 unique (R_{int} = 0.0397, R_{sigma} = 0.0252) which were used in all calculations. The final R_1 was 0.0350 (I > 2σ(I)) and wR_2 was 0.0963 (all data).

Crystal data for $PPh_2C(=O)NH(^t Bu)$ (3h)

$C_{17}H_{20}NOP$ (M = 285.31 g/mol): triclinic, space group P-1 (no. 2), a = 10.1317(3), b = 10.5022(4), c = 14.6490(6) Å, α = 87.932(3), β = 89.517(3), γ = 89.127(3)°, V =

1557.48(9) Å^3, Z = 4, T = 120(2) K, μ(Cu-$K\alpha$) = 1.515 mm^{-1}, D_{calc} = 1.217 g/cm^3, 11349 reflections measured (8.426° ≤ 2Θ ≤ 147.656°), 6080 unique (R_{int} = 0.0347, R_{sigma} = 0.0435) which were used in all calculations. The final R_1 was 0.0343 ($I > 2\sigma(I)$) and wR_2 was 0.0917 (all data).

Crystal data for $PPh_2C(=O)N(Ph)C(=O)NH(Ph)$ (4a)

$C_{26}H_{21}N_2O_2P$ (M = 424.42 g/mol): orthorhombic, space group $P2_12_12_1$ (no. 19), a = 5.9842(2), b = 10.9578(5), c = 31.8272(12) Å, V = 2087.01(15) Å^3, Z = 4, T = 120(2) K, μ(Cu-$K\alpha$) = 1.377 mm^{-1}, D_{calc} = 1.351 g/cm^3, 5909 reflections measured (5.554° ≤ 2Θ ≤ 147.524°), 3561 unique (R_{int} = 0.0515, R_{sigma} = 0.0652) which were used in all calculations. The final R_1 was 0.0597 ($I > 2\sigma(I)$) and wR_2 was 0.159 (all data).

Crystal data for $PPh_2C(=O)N(^pTol)C(=O)NH(^pTol)$ (4b)

$C_{28}H_{25}N_2O_2P$ (M = 452.47 g/mol): monoclinic, space group $C2/c$ (no. 15), a = 26.103(3), b = 5.7961(5), c = 32.100(4) Å, β = 104.115(11)°, V = 4710.0(9) Å^3, Z = 8, T = 119.97(12) K, μ(Cu-$K\alpha$) = 1.251 mm^{-1}, D_{calc} = 1.276 g/cm^3, 27055 reflections measured (6.984° ≤ 2Θ ≤ 151.008°), 4797 unique (R_{int} = 0.0917, R_{sigma} = 0.0497) which were used in all calculations. The final R_1 was 0.0779 ($I > 2\sigma(I)$) and wR_2 was 0.232 (all data).

References

1. H. R. Sharpe, A. M. Geer, H. E. L. Williams, T. J. Blundell, W. Lewis, A. J. Blake and D. L. Kays, *Chem. Commun.* **2017**, *53*, 937-940.
2. D. L. Kays (née Coombs) and A. R. Cowley, *Chem. Commun*., **2007**, *10*, 1053-1055.
3. A. C. Behrle and J. A. R. Schmidt, *Organometallics,* **2013**, *32*, 1141-1149.
4. J. Cosier and A. M. Glazer, *J. Appl. Crystallogr.*, **1986**, *19*, 105-107.
5. CrysAlisPRO Oxford Diffraction/Agilent Technologies UK Ltd Yarnton England.
6. G. M. Sheldrick, *Acta Crystallogr. Sect. C Struct. Chem.*, **2015**, *71*, 3-8.
7. G. M. Sheldrick, *Acta Crystallogr. Sect. A Found. Crystallogr.*, **2008**, *64*, 112-122.
8. G. M. Sheldrick, *Acta Crystallogr. Sect. A Found. Crystallogr.*, **2015**, *71*, 3–8.
9. O. V Dolomanov, L. J. Bourhis, R. J. Gildea, J. A. K. Howard and H. Puschmann, *J. Appl. Cryst*, **2009**, *42*, 339-341.
10. http://checkcif.iucr.org/